THE BEHAVIORAL EFFECT OF LABORATORY TURBULENCE ON COPEPODS

A Thesis
Presented to
The Academic Faculty

by

Katherine Denise Rasberry

In Partial Fulfillment
of the Requirements for the Degree
Master of Science in Civil Engineering

Georgia Institute of Technology
August 2005

THE BEHAVIORAL EFFECT OF LABORATORY TURBULENCE ON COPEPODS

Approved by:

Dr. Donald R. Webster, Chair
School of Civil and Environmental Engineering
Georgia Institute of Technology

Dr. Jeannette Yen
School of Biology
Georgia Institute of Technology

Dr. Philip J. W. Roberts
School of Civil and Environmental Engineering
Georgia Institute of Technology

Date Approved: July 8, 2005

ACKNOWLEDGMENTS

I want to thank my advisor, Dr. Donald Webster, for being a mentor to me for almost three years. His support and guidance have been an inspiration. I am truly blessed to work with such a wonderful advisor.

Special thanks go to Dr. Jeannette Yen for helping me with my experiments and teaching me how to work with animals. Her positive attitude and enthusiasm were always appreciated.

I appreciate the support and friendship from the graduate students in my department. A special thanks to Kim Catton and Brock Woodson for assisting me with data analysis.

Leigh, thank you so much for the illustration. I am so happy that you could be a part of my work here at Georgia Tech, and I am so grateful for your friendship and wisdom.

I want to thank my family for being so supportive. Mom and Dad, none of this could have happened without you. Your love and guidance mean so much to me.

Copepods Moving Toward the Light
Leigh Margaret Pearson, June 2005

TABLE OF CONTENTS

LIST OF TABLES

LIST OF FIGURES

SUMMARY

Copepod species are distributed throughout the ocean by many factors, including chemical, biological, and physical effects. Turbulence in the ocean has been suggested as a factor that vertically partitions some species of copepod. Copepods may seek calmer waters by sinking to deeper levels as the surface waters become more turbulent, or may maintain their position in turbulent waters. The goal of this study is to determine the behavioral effects of turbulence on three species of copepod, *Calanus finmarchicus*, *Acartia tonsa*, and *Temora longicornis*.

Experiments consisted of exposing each of the species to stagnant water plus four levels of turbulence intensity. The experiments were conducted in a laboratory apparatus that mimics oceanic turbulence. The turbulence characteristics have been previously characterized by particle image velocimetry (PIV), that show the turbulence to be nearly isotropic and homogeneous in the observation region. Behavior responses were quantified via several measures, including the number of animals phototactically aggregating per minute, the number of escape events, the swimming speed, and the net-to-gross-displacement ratio. There are important conclusions about the effect of laboratory turbulence on copepods. The size of the copepod has a significant effect on its aggregation and swimming capability with increasing turbulence. The smaller copepods had less ability to overcome a strong flow field, and they were more likely to be advected by the stronger flow fields. Swim style also can influence how a copepod reacts to increased turbulence. If the copepod is a hop and sink traveler, then the copepod

continues to hop and sink more than its cruising counterparts as turbulence increases. The cruise and sink travelers did not alter the number of escapes in response to turbulence.

CHAPTER I

INTRODUCTION AND OBJECTIVES

Copepods in pelagic ecosystems are subject to turbulent flow motions. It has been observed that some copepods travel to deeper depths in the water column during turbulent events at the surface, while others prefer the chaotic flow pattern at the surface (Mackas et al. 1993, Lagadeuc et al. 1997, Mauchline 1998, Incze et al. 2001, Visser and Stips 2002, Yamazaki et al. 2002). The behavior of copepods is thereby altered during higher levels of turbulence. In order to test the behavior of individual copepods, three species: *Acartia tonsa*, *Calanus finmarchicus*, and *Temora longicornis*, were monitored in a laboratory turbulence generator (Webster et al. 2004). The goal of this research is to make detailed, high resolution observations of copepod behavior response to different levels of turbulence.

Copepods possess setae that facilitate mechanosensing of the local velocity field. In laboratory experiments copepods are known to escape more frequently for high levels of strain rate (Fields and Yen 1997). These observations were made for steady laminar flow conditions that were created to mimic predator flow patterns. The response to a chaotic velocity field with fluctuating levels of strain rate is essentially unknown. In this study, copepod behavior will be analyzed in an isotropic turbulent regime. The turbulence generator provides a well-quantified, nearly isotropic and homogeneous turbulent flow at low Reynolds numbers. The turbulence characteristics previously have

been characterized by particle image velocimetry (PIV, Brathwaite 2003, Webster et al. 2004). Copepods will be monitored for four levels of turbulence plus stagnant water.

Behavioral analysis will include looking for motion that indicates a preference of turbulence levels. The hypothesis to be tested in this thesis is that copepods exhibit species-specific behavior responses to turbulence. This research focuses on aggregation toward a light source, swim speed, net-to-gross-displacement ratio (NGDR), and escape behavior of the copepod. Copepod response variation could be due to differences in size, diet, mating patterns, and migratory patterns of the species. The objective is to test whether the three species of copepod react differently in the five turbulent regimes.

CHAPTER II

LITERATURE REVIEW

2.1 Overview on Copepods

Coastal marine microzooplankton are a taxonomically diverse assemblage of organisms often composed of ciliated protozoans, rotifers, and crustaceans. Copepods (meaning "oar foot") are aquatic crustaceans, primarily inhabiting marine environments. Copepods are usually 0.5-2.0 mm in length, while a few marine species are one centimeter in length (Mauchline 1998). Figure 2.1 provides a sketch of a copepod. Many copepods are phototactic, which means they can differentiate between light and dark and are often attracted to light. Copepods eat bacteria, diatoms, and other tiny, single-celled organisms in the water (Mauchline 1998). Figure 2.2 shows a photograph of a copepod.

Copepods are probably the most numerous multicellular organisms on earth. While more numerous than insects, they are not as diverse; there are 200 families, 1,650 genera, and 11,500 species of copepod (Mauchline 1998). Many copepods are parasites of fish, while the others are free swimming. Copepod habitats are known to include fresh water streams, rivers, and lakes, subterranean caves, sediment layer in the open ocean, hypersaline conditions, and even rainwater collected in bromeliad leaves or leaf litter on the ground. Their habitats also range from the highest mountains to the deepest ocean trenches and from the cold polar ice-water interface to the hot active hydrothermal vents (Mauchline 1998). They are most abundant in the Arctic and Antarctic Oceans and also inhabit continental shelves in the middle latitudes (Mauchline 1998).

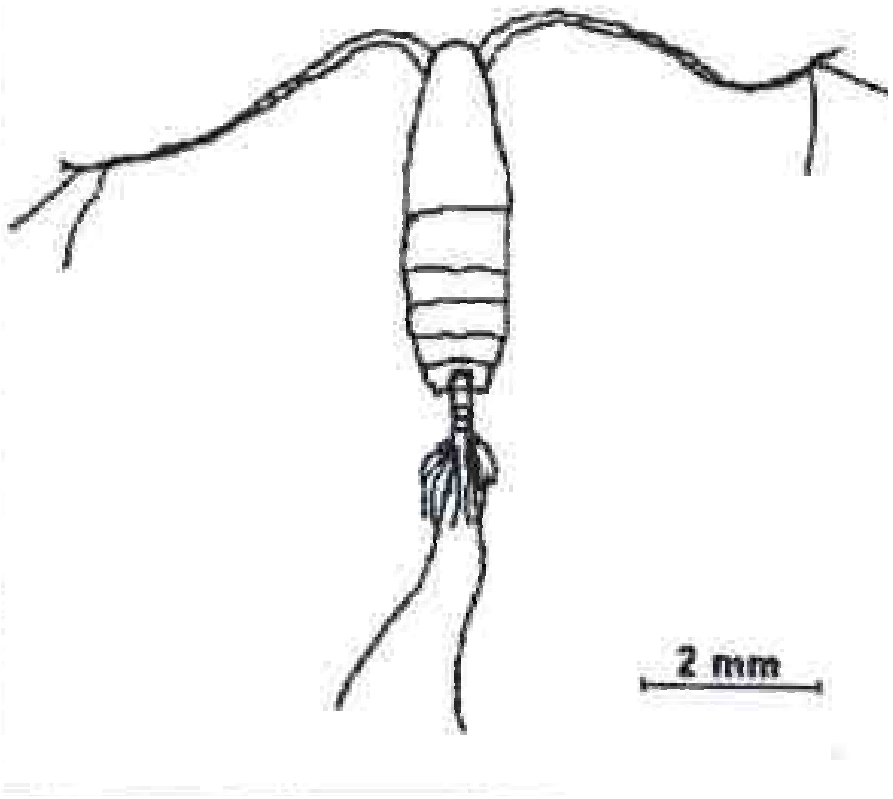

Figure 2.1 Sketch of a copepod with length scale. (Source: Mackas et al. 1993.)

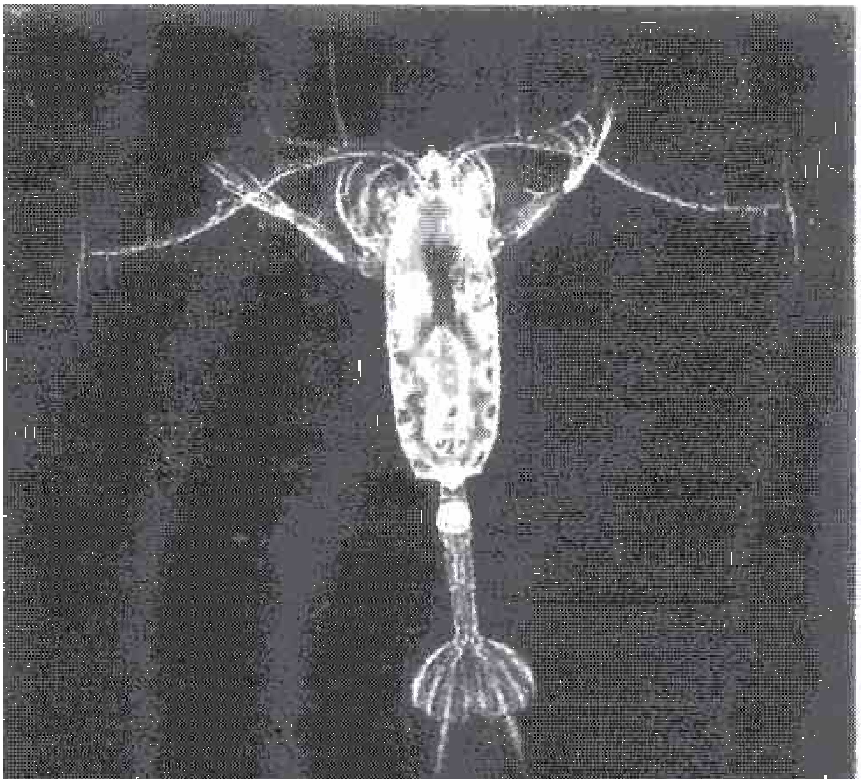

Figure 2.2 Photomicrograph of a live copepod, *Euchaeta norvegica.* (Source: Yen and Strickler 1996).

Copepods are important links in marine food webs, transferring large amount of carbon to higher trophic levels. Copepods feed on phytoplankton and hence play a pivotal role in marine food webs as phytoplankton grazers and active predators (Mauchline 1998). Many organisms, including a variety of invertebrate species, mussels, fish and fish larvae, squid, sea birds, and mammals (such as baleen whales and some seals) eat free-swimming copepods. Copepods are at the small end of the spectrum of prey for baleen whales, but sei, bowhead, right, and fin whales consume large quantities of them in the North Atlantic, North Pacific, and Antarctic Oceans (Mauchline 1998). Larval stages of many commercially-important fish species also prey primarily on copepods, and thus copepod abundance may directly affect the recruitment success of these fish.

Predation acts as a major force controlling the dynamics and structure of planktonic communities. The ability of prey to avoid predation is crucial and the selection for offenders is swift (Fields and Yen 1997). Predation exerts considerable influence on the structure of lower trophic level communities and offers insight into evolutionary control. The effects of predation within an ecosystem can vary in both time and space (Mauchline 1998). Calanoid copepods can affect the density of their prey because of their large numbers. For instance, they can limit the duration of a phytoplankton bloom through grazing it at a higher rate than the rate of production of phytoplankton. Additionally, they can affect their own or another species populations by grazing on available eggs and nauplii (Mauchline 1998).

2.2 Copepod Distribution in the Water Column

Copepods are found at depths from the ocean surface waters to the ocean floor; however, they vary in population density. In the upper 200-300 meters the density of copepods is about 20-60 individuals/m^3. The number decreases to a few individuals/m^3 at 1000 meters depth. At 8000 meters depth, the number of individuals has decreased to 5-13/100 m^3 (Mauchline 1998).

Individuals within populations of copepods are not randomly distributed in the water column. They are influenced by the physical and chemical characteristics of their environment (Mauchline 1998). One physical characteristic that appears to affect copepod distribution is turbulence. Waves, currents, and tides interact in the ocean to create highly complex flow conditions, including the production of turbulence. Turbulence consists of disorderly, unpredictable, and chaotic flow motions. Turbulence in the ocean occurs over a wide range of scales from large-scale global circulation to diffusive microscales (e.g. Jiménez 1997) and the turbulence intensity varies both spatially and temporally. At the scale of zooplankton (order of millimeters), the character of oceanic turbulence is generally isotropic, which means the turbulent fluctuations are, on average, independent of direction (Webster et al. 2004). These small animals are subject to the fluctuating fluid forces imposed by the turbulent velocity field. Turbulence patchiness, therefore, is likely to affect microscopic animals such as copepods and larval fish. In fact, the vertical variation of turbulence exerts an influence on vertical migratory behavior copepods (Mackas et al. 1993, Lagadeuc et al. 1997, Incze et al. 2001, Visser and Stips 2002). It appears that some copepods prefer a more turbulent environment in

the upper mixing layer, while others are found in deeper, calmer waters (Yamazaki et al. 2002).

Several field studies support the hypothesis that turbulence avoidance behavior can lead to enhanced subsurface concentrations. Mackas et al. (1993) sampled the waters of the sub-arctic Pacific during spring. They found that the copepods were stratified in two layers with two species per layer. The upper layer corresponded to the mixing layer, while the lower layer was the weaker, non-mixing layer. Mackas et al. (1993) present two possible explanations: copepods either have different trophic roles or they have preferences in turbulence levels. Incze et al. (2001) sampled the water near Georges Bank off the northeastern coast of the United States. Most copepods were found in regions of lower turbulence. This study showed that copepodites and copepod nauplii were most abundant in the upper twenty meters, and very few were found below twenty-five meters. Most copepod life stages inhabited shallower depths of ten to fifteen meters when the surface was calm compared to more turbulent conditions. There was a downward movement of most copepods during a high wind event and a rapid return to shallower depths afterward. Franks (2001) claims the significant benefit of a turbulence avoidance mechanism is that the organisms would be feeding in a calmer environment. Organisms that would most benefit from the turbulence avoidance behavior are those that can swim fast enough to exit the mixing layer on a relevant time scale and that eat prey that also shows this behavior.

Visser et al. (2001) sampled copepods in the North Sea in order to study their vertical distribution. The authors hypothesized that zooplankton seek the water depth with turbulence level and food concentration that maximizes feeding opportunities and

minimizes predation risk. The goal was to test whether theoretical and lab studies of copepod feeding translate into observable effects in nature, and/or whether vertical migratory behavior of copepods is modified by the effects of turbulence. Wind is generally the cause of near-surface turbulence and the turbulent energy dissipates to deeper water. The copepods sampled in this study were mostly *Oithona similis*. It was found that copepods descended in the water column during periods of strong turbulence. When the turbulent velocity approaches feeding-current velocity, the feeding current may become significantly eroded and thus affect feeding rate negatively. Therefore, turbulence has a negative effect on food acquisition in suspension-feeding copepods. Ambush-feeding copepods are expected to enjoy the largest benefit from elevated ambient turbulence in terms of feeding rates because turbulence may interfere with hydromechanical predator perception thus reducing the ability of prey to escape. It was found that copepods in general descend during wind events.

Copepod distribution is also affected by other physio-chemical characteristics including phytoplankton density, light level, and copepod density. Zooplankton aggregation appears to be influenced by a variety of factors such as physical features, odors, and food (Yen and Bundock 1997). Because copepods are phototactic, they are often found in dense swarms in the light between mangrove tree roots and coral reefs (Ambler et al. 1991). Leising and Yen (1997) studied the behavior of light-induced copepod swarms. They found that as the density of the swarm increased, the average nearest neighbor distance (NND) decreased; as did the mean minimum NND. While occasional physical contact may occur, resulting in escapes or attempted mating, it appears that most swarm members remain outside the field of self-generated fluid motion

in the boundary layers surrounding their neighbors. Leising and Yen (1997) divided the aggregating swarm into three zones. In Zone 1, closest to the light, the high population density caused escapes and sinks. In Zone 2, there was a lower encounter rate, fewer escapes, and an equal amount of sinking and swimming toward the light. In Zone 3, farthest from the light, there was the greatest amount of swimming toward the light. Without communication, swarming members may orient themselves only to attractant or they may show some attraction or orientation to other members as well as attractant, and may alter their swimming patterns accordingly (Yen and Bundock 1997). Local orientation in zooplankton may be along streamlines in the flow field surrounding swimming or feeding neighbors (Yen and Bundock 1997). Copepod density is extremely important in determining the survival of fish larvae, which prey on copepods. Copepod density varies seasonally in the middle latitudes because of phytoplankton blooms. In the spring, the phytoplankton production increases in the North Atlantic. This is called the spring bloom (Mann and Lazier 1996). The spring bloom creates an increase in zooplankton. In the Pacific there is a gradual increase of phytoplankton, accompanied by zooplankton, from mid-winter to mid-summer (Mann and Lazier 1996).

2.3 Hydrodynamical Sensory Ability of Copepods

Copepods sense water movement via mechanosensors along its antennules, which are called setae. Fields and Yen (1996) suggest that setal bending is the mechanism by which copepods transform the motion of a flow pattern into a neurophysiological signal that elicits behavior. Fields et al. (2002) state that the physiological response of all setae

tested showed strong correlation to both angular displacement and angular velocity of the water (Figure 2.3). Figure 2.4 shows a detailed sketch of the copepod antennules.

There are several flow motions (or hydrodynamic cues) that may elicit a behavior response in copepods. These include velocity, acceleration, vorticity, and deformation (strain) rates. Fields and Yen (1997) reported that shear strain rate was found to be the least variable characteristic eliciting the escape reaction and best explained the observed pattern of escapes. Their experiment consisted of observing the escape response in a laminar siphon flow. There was a lack of escapes in the region directly above the siphon (the region with the highest water speed), and a cluster of escapes lateral to the mouth of the siphon (the region with the highest shear strain rate). This shows that flow speed is not an adequate indicator of prey escape location.

Kiørboe et al. (1999) observed *Acartia tonsa* in a Couette tank, a rolling tank, a suction pipette, and an oscillating chamber. Their observations did not fully support the hypothesis that the threshold intensity of a particular velocity gradient component depends solely on the signal strength (velocity difference) it causes. The ability of copepods to perceive fluid deformation rates and remotely detect predators reduces their risk of being eaten, but does not eliminate it. Deformation rate is generally the most significant component for predator and prey perception (Kiørboe and Visser 1999).

Virtually all copepods exhibit an escape reaction to an apparent predation risk (Fields and Yen 1997). Viitasalo et al. (1998) compared the susceptibilities of two copepod species to predation. It was found that slow fish were more successful at catching prey than the faster fish. This suggests that faster fish create a larger disturbance in the water; therefore, they are easier to detect and avoid. Also, there are important

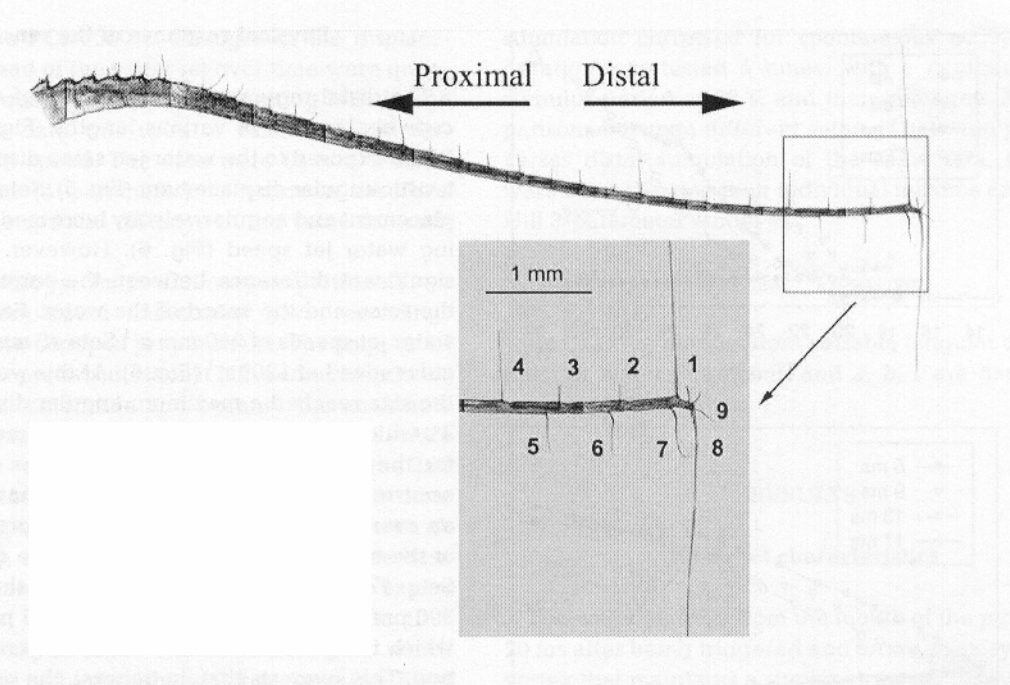

Figure 2.3 Photograph of the right antennule of *Gaussia princeps* (Source: Fields et al. 2002).

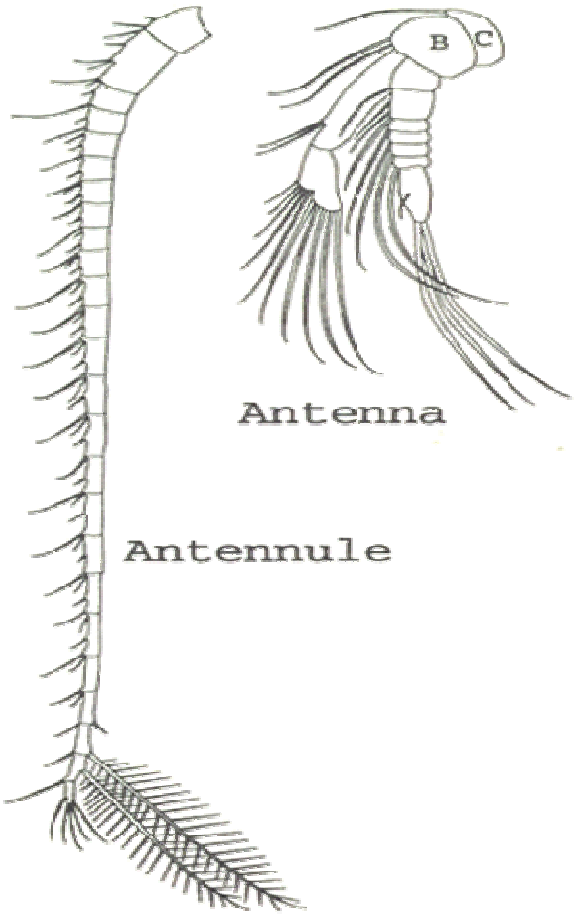

Figure 2.4 Detailed sketch of antenna and antennule. (Source: Mauchline 1998).differences between escape capabilities of copepod species. The swimming mode and the approaching skill of predators are important for their foraging success.

It is important to note that previous observations of copepod response to flow motion have been performed for contrived laminar flows. Thus, the instantaneous behavioral response to fluctuating turbulent motions is unknown.

2.4 Effect of Turbulence on Copepods

Copepods do not necessarily passively drift with the ambient flow. Plankton with swimming speeds substantially higher than the turbulent velocity fluctuations can be expected to exhibit motion independent of the surrounding flow. Plankton with swimming speeds less than turbulent velocity fluctuation can be expected to be swept along with the flow. Yamazaki and Squires (1996) examined three species of copepod and found that all three could swim faster than the surrounding turbulent flow.

On the individual level, turbulence plays a role in predator-prey encounter rates, mating, and the survival of the copepod. For instance, at plankton contact scales turbulence is homogenous and isotropic and possesses velocities comparable to those of the plankton. It has been suggested that increased turbulence intensity increases the encounter rate (Rothschild and Osborn 1988). Microscale turbulence increases planktonic prey contact rates because turbulent fluid motion increases the velocity difference between predators and their prey (Kiørboe and Saiz 1995). Titelman and Kiørboe (2003) studied two modes of travel exhibited by copepods: jump-sink and cruise. They showed that the jump-sink copepods experience a risk of encountering a predator an order of magnitude higher than the cruisers. However, the jump-sink copepods are better at detecting hydrodynamic signals than the cruisers. Cruising copepods that generate weak hydrodynamic signals and have modest predator encounter

rates are poor at detecting predators remotely. Prey becomes more easily detected, either visually or vibrationally, with increased activity (Buskey et al. 1993). Zooplankton prey can limit both detection and encounter with predators by reducing their motility (Titelman 2001). By spending more time moving at low velocity, e.g. sinking, prey may reduce the hydrodynamic signal that can be perceived by a predator, and thus limit their exposure. For example, *T. longicornis* nauplii require a higher flow deformation rate than *A. tonsa* nauplii to elicit an escape response (Titelman 2001). This implies that *A. tonsa* may respond to a potential predator at a greater distance away than *Temora*.

Saiz and Alcarez (1992) studied the behavior of the copepods species *A. tonsa* under turbulent conditions. Turbulence was generated by a small Netlon grid (0.5 cm mesh size) placed vertically in an experimental aquarium. The grid was attached to a vibrating rod. They observed that the *A. tonsa* sank passively through the water and displayed frequent rapid upward bursts of swimming to maintain its depth position in calm water. Under turbulent conditions there was a significant difference in their performance, and the current carried the copepods away. The copepod's jump frequency and jump speed were faster under turbulent conditions.

Acartia tonsa is one of the most studied copepod species inhabiting neritic and estuarine water. Saiz (1994) tested the effects of turbulence and food concentration on the feeding behavior on *A. tonsa*. The experiment was conducted using two tanks, one with still water and one with turbulent water. Three food concentration levels were used to compare the behavior in the tanks. In still water *A. tonsa* spent 78-99% of its time in feeding bouts. The percentage decreased from low to high food concentration. The turbulence did not affect the proportion of time spent in feeding bouts at either low or

high food concentrations. The frequencies of feeding bouts and jumps did not differ significantly between still and stirred conditions. At high food concentration, turbulence did not induce any changes. *A. tonsa* reacts to different food concentrations by allocating less time to feeding at very low and high food concentrations and mainly by changing the duration of feeding bouts, spending more time in long feeding bouts at low food concentrations.

Similarly, Saiz and Kiørboe (1995) observed the feeding of *Acartia tonsa* in turbulent environments. They state that the ambush-feeding copepods substantially enhance their feeding rates in turbulent environments, and suspension-feeding copepods are only marginally affected at realistic intensities of turbulence.

Saiz et al. (2003) reported on the effects of small scale turbulence on the copepod *Oithona davisae*. Six independent feeding experiments were conducted, each consisting of a calm treatment (no turbulence) and a turbulent treatment (one of six turbulent intensities). The six levels of turbulence ranged from realistically low to high values for coastal and shelf waters. The highest level was extreme and only found occasionally in nature. Small-scale turbulence affects the feeding of the ambush copepods *O. davisae*. Positive net effects on feeding were evident only at the lowest turbulence intensity tested, which is comparable to values found in low-energy marine environments. In higher turbulence levels there was either no net effect or impairment of feeding. This finding is consistent with field observations of *Oithona*, which appear to avoid high turbulence layers. Overall, these observations agree with the theory provided by Kiørboe and Saiz (1995), which predicts a major effect of turbulence on ambush copepods at low and moderate turbulence intensities and negligible effects on suspension feeders. Other

ambush species studied, *Acartia tonsa* and *Calanus typicus,* have the ability to create feeding currents as well, being able to switch into suspension feeding strategies, if needed. Dual-mode foragers might not rely as much on mechnosensory array, therefore should be able to cope with higher turbulence intensities. It appears that the higher sensitivity of *O. davisae* feeding to turbulence would help explain field observations of the deepening of *Oithona* vertical distribution under situations of high turbulence.

2.5 Summary

Copepods use mechanosensors called setae to perceive local fluid motion. The setae bend and the copepod can react to the detected fluid movement. The movement might be induced by prey, for which the copepod would attack, or it could be induced by a predator, hence causing an escape reaction.

Turbulence also appears to affect copepod behavior. The fluctuating strain rate associated with turbulent flow motions causes the copepod's setae to bend, therefore causing a reaction. It has been shown that some copepod species retreat into deeper water when the turbulence intensity increases and then climb to their original position when the turbulence intensity dissipates.

A hypothesis is formed that states: individual copepod response to turbulence leads to vertical partitioning of the species. In order to test this hypothesis, copepods from the Gulf of Maine will be tested to see how they react to turbulence. Using a laboratory apparatus to generate natural turbulent conditions, copepods will be observed for four levels of turbulence in addition to stagnant water conditions. The copepods will be analyzed for swim behavior, escape reactions, and swim speeds. Testing copepod

behavior in turbulent water can illuminate how and why the copepods respond to specific turbulent flow motions and provide insight into the vertical partitioning observed in the ocean.

CHAPTER III

EXPERIMENTAL EQUIPMENT AND PROCEDURES

The experiments, conducted in the Cherry Emerson Building at the Georgia Institute of Technology, focused on the behavior of copepods, *Acartia tonsa, Temora longicornis,* and *Calanus finmarchicus*, in turbulent waters. The experiments were performed for five flow conditions: stagnant water plus four intensity levels of turbulence. The data collected was analyzed for behavioral patterns including escape response, aggregation toward light, and swim speed.

3.1 Physical Environment

The experiments were conducted in a dark laboratory room. The windows were covered with aluminum bubble wrap to prevent ambient light interference with the cameras and laser. The room temperature was approximately 22 °C. To mimic the animals' natural habitat, the water was chilled to 12 °C prior to the experiment. During the course of the experimental observations (3 hour duration) the water temperature increased to 13 °C. All experiments were conducted during daylight hours.

The apparatus used in the experiments was the turbulence generator (T-box) described by Brathwaite (2003) and Webster et al. (2004). The inner dimensions of the T-box were 0.4 m × 0.4 m × 0.4 m. The size was large compared to the copepods but small enough to use in the laboratory. The apparatus was filled with approximately 50 L of artificial seawater created with filtered fresh water and Instant Ocean. The salt

concentration was 30 ppt, which was consistent with habitats of the copepods tested. A sketch of the chamber and actuators is shown in Figure 3.1. The six sides of the cube and eight corners were Plexiglas sheets (1.9 cm thick). Optical access was equally available from all four Plexiglas sidewalls. The corners of the T-box were mechanically secured with machine screws and acrylic glue. All components were either acrylic or 316 stainless steel in order to prevent corrosion in saltwater and to create a biologically-habitable environment. The chamber was accessed through the round opening (15 cm diameter) at the top of the tank. The opening was surrounded by a 5 cm tall Plexiglas berm that holds extra water (e.g. the water displaced by objects temporarily submerged in the tank). A Plexiglas lid fit securely into the opening to seal the chamber during experiments. A drain pipe (1.3 cm diameter) was located at the bottom of the chamber. The T-box was supported by a steel stand (60 cm high, shown in Figure 3.2).

Four turbulence levels were used in the experiments that correspond to dissipation rates that match coastal and wind-driven turbulence regions. A velocity time series for any location in the turbulent flow appeared "random" and "chaotic." The exact instantaneous velocity cannot be predicted, but the overall behavior was described stochastically and possessed certain universal characteristics (Webster et al. 2004). Brathwaite (2003) demonstrated that the turbulent flow fields produced by the turbulence generator were statistically nearly homogeneous and isotropic. However, zooplankton are likely to respond to the instantaneous flow field instead of a time-average value (Fields et al. 2002). The velocity and strain rate components fluctuate in an unpredictable manner and expose zooplankton to unsteady advection and mechanosensory stimulus.

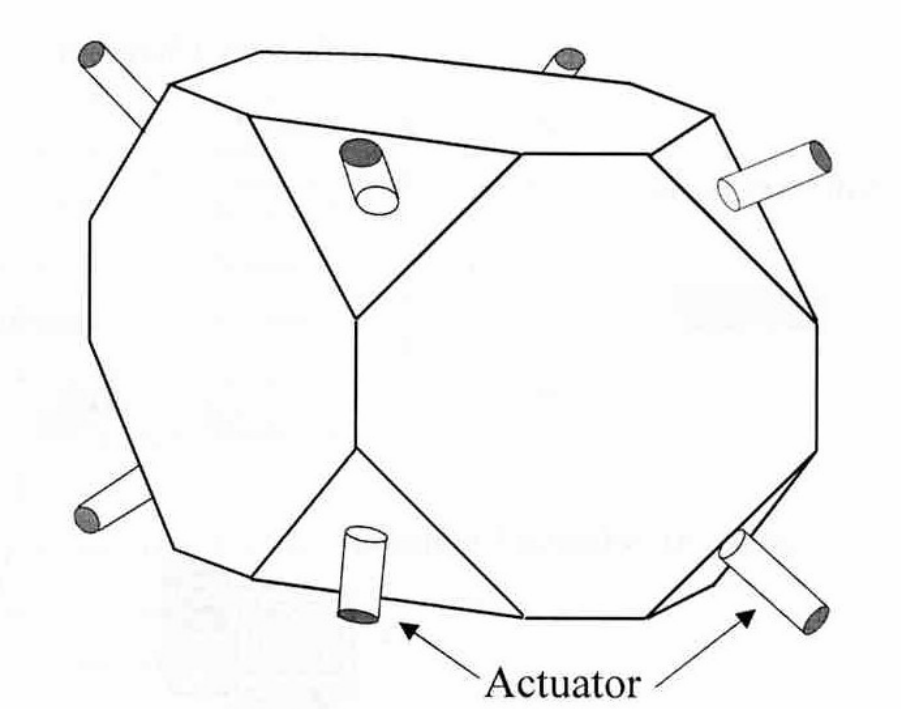

Figure 3.1 Sketch of turbulence apparatus (Brathwaite 2003).

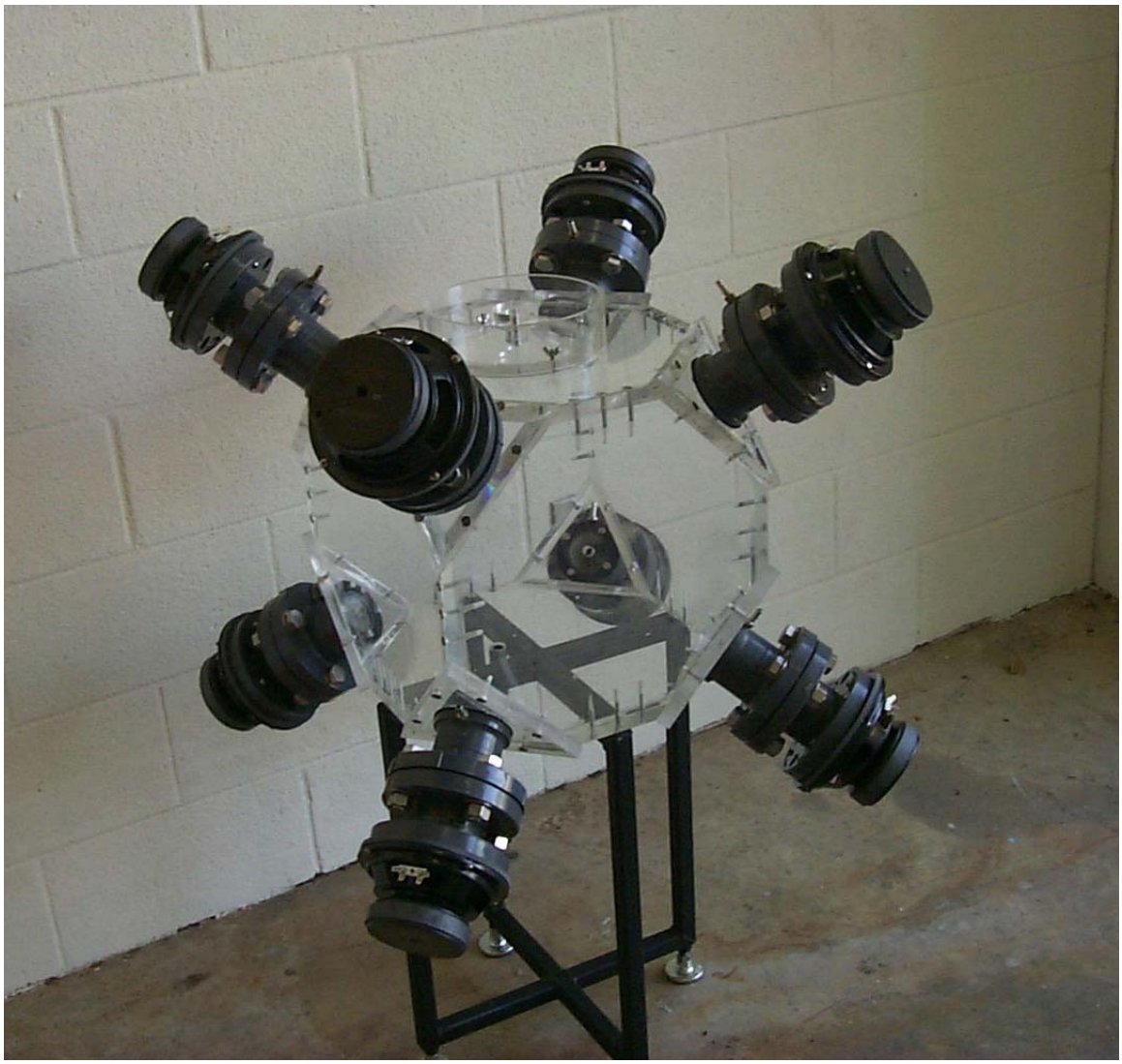

Figure 3.2 Photograph of the turbulence chamber and actuators (Webster et al. 2004).

Synthetic jet actuators, located at each corner of the T-box, generate the turbulent flow. The oscillating diaphragm in the synthetic jet actuator alternatively drew fluid into and expelled fluid from the actuator chamber to produce net-zero-mass-flux turbulent jets. The eight synthetic jet flows intersected at the apparatus center. The flow field at the center of the box was statistically isotropic and homogeneous (Webster et al. 2004). The actuators were driven by a low-power sinusoidal voltage signal that was generated with a National Instruments DAQCard installed in a laptop computer. The sinusoidal signal was divided into eight signals that were individually amplified via an eight channel power amplifier. The frequency and amplitude of the signal controlled the jet strength and hence the turbulent flow intensity in the apparatus. The apparatus is shown in Figures 3.1 and 3.2.

For T0, the actuators were stationary and no active turbulent forcing was present, hence the fluid was essentially stagnant. For T1, T2, T3, and T4, the turbulence intensity was set by using pre-determined amplification settings for each of the eight actuators. Table 3.1 shows the dissipation rates (ε) and root mean square (r.m.s.) velocities for each turbulence level reported in Webster et al. (2004). The dissipation rate is often used in the oceanography literature to describe the turbulence intensity. With this apparatus, the turbulence intensity spans more than 2 orders of magnitude.

Table 3.1 Dissipation rate and root mean square velocity for the four turbulence intensity levels (Webster et al. 2004).

Turbulence Level	**1**	**2**	**3**	**4**
ε **(cm^2/s^3)**	0.002	0.009	0.096	0.25
Velocity r.m.s. (cm/s)*	0.11	0.28	0.75	0.93
Strain Rate r.m.s. (1/s)	0.11	0.24	0.79	1.15

*Velocity r.m.s. is the average of the measured r.m.s. for each coordinate direction

3.2 Copepods tested

Three species of copepod were tested during the course of these experiments: *Acartia tonsa, Temora longicornis*, and *Calanus finmarchicus*. Tables 3.2 and 3.3 provide characteristics for the copepod species and collection information.

Table 3.2 General characteristics of copepods tested.

Species	Bodylength (mm)	Swim Speed (mm/s)	Sinking Rate (mm/s)	Habitats	Geography	Swim Style
Acartia tonsa	1-2	1-10[a] 2-8[b] 3-5[c]	0.99[f] 0.6-0.8[g]	Coastal Estuaries	World	Hop and Sink
Temora longicornis	1-3	2.7-6.1[d]	2.9[h] 2.5[g]	Continental Shelf	Atlantic, Pacific	Cruise and Sink
Calanus finmarchicus	4-5	2.0-5.0[d] 10[e]	5[h] 1.9-2.2[i] 2.3-3.1[i] 0.8-3.5[i]	Continental Shelf	N. Atlantic	Cruise

[a] Mauchline—Buskey (1994)
[b] Mauchline—Buskey et al. (1986)
[c] Mauchline—Tiselius (1992)
[d] Mauchline—Buskey and Swift (1985)
[e] Mauchline—Hirche (1987)
[f] Mauchline—Jacobs (1961)
[g] Mauchline—Jonsson and Tiselius (1990)
[h] Mauchline—Apstein (1910)
[i] Mauchline—Gross and Raymont (1942)

Table 3.3 Collection information for copepods tested.

Species	Collection Method	Date Collected	Date of Experiment	Collector	Location
Acartia tonsa	200 μm net, tow	January 13, 2005	February 7, 2005	SUNY-Stony Brook	Long Island Sound
Temora longicornis	200 μm net, tow	April 21, 2004	April 23, 2004	UNH	Gulf of Maine
Calanus finmarchicus	200 μm net, tow	February 24, 2004	February 26, 2004	UNH	Gulf of Maine

The copepods' natural habitat transmits light differently depending on wavelength. Cohen and Forward (2002) report that estuarine waters transmit maximally at longer wavelengths (~580 nm), coastal waters transmit at slightly shorter wavelengths

(~500 nm), and clear ocean water transmits at even shorter wavelengths (~470nm). The ambient wavelength that occurs at twilight in coastal habitats is 480 to 620 nm (Cohen and Forward 2002).

Acartia tonsa is positively phototactic (Stearns and Forward 1984). *A. tonsa* is capable of phototactically responding to a broad range of wavelengths (380 to 700 nm). However, *A. tonsa* is maximally sensitive over a more narrow spectral range (~453 to 620 nm). Buskey et al. (1989) reported that *A. tonsa* moved toward a directional source of light, whereas Shallek (1942, 1943) found that *A. tonsa* sank in light that is not highly directional. Stearns and Forward (1984) concluded that the spectral sensitivity of *A. tonsa* is adapted for vertical migration in estuarine areas. Furthermore, *A. tonsa* exhibits behavior that follows the diurnal cycle (Buskey et al. 1989). At sunrise, the increasing light intensity causes downward migration. For *A. tonsa*, this behavior may result from an increase in time spent sinking between hops rather than active downward swimming. When the organisms reach the bottom they adapt to that particular light level. At sunset, the decrease in light intensity causes upward migration.

Other calanoid copepods respond in a similar manner as *A. tonsa*. Cohen and Forward (2002) studied the photactic behavior for four coastal species of calanoid copepods. They found that *Centropages typius*, *Anomalocera ornata*, and *Calanopia americana* responded to a range of wavelengths that matched the ambient wavelengths (480-520 nm), while the surface dweller, *Labidocera aestiva*, had photo-responses over a greater range of wavelengths.

3.3 Behavior Observation Method

The box was filled with approximately 30 ppt saltwater until it was two-thirds full. Before adding water to the T-box a rubber stopper was placed in the drain at the bottom of the tank to prevent mixing of water from the drain pipe into the chamber. The copepods were added slowly to prevent injuries and fatalities. Additional saltwater was added to the box until the chamber was completely full. Air bubbles were removed by bleeding the actuators and wiping a squeegee on the top and sides of the box. The lid was placed on the box.

A light beam was projected vertically through the center of the box in order to aggregate the copepods. The light source is the green line (514 nm) of a 100 milliWatt laser (Uniphase model No. 2201-100ML). This wavelength is in the spectrum range for natural habitats and within the spectrum range for which copepods show phototactic behavior. The laser head, emitting a horizontal beam, was placed next to and below the T-box. A small gold mirror redirects the beam vertically through the turbulence apparatus. A hole (0.95 cm diameter) was drilled in the support stand to allow the laser beam to pass through the center. The beam trajectory in the T-box was nearly vertical (within 2°).

A shadowgraph system was used for recording copepod position. A shadowgraph is an image produced by casting a shadow on a screen. A translucent sheet of paper (100% rag vellum) was taped to the outsides of each wall of the T-box facing the cameras. These sheets acted as the screen for the shadow images of the copepods. Illumination is provided by lasers operating in the red wavelengths, for which the tested copepods do not behaviorally respond. Opposite from the cameras a Melles-Griot red

diode OEM laser was expanded and collimated by reflection off circular concave mirrors (Melles-Griot, 2000 mm focal length, 153 mm diameter, f/10) creating a wide column of laser light through the box center (Figure 3.3). During the *C. finmarchicus* and *T. longicornis* experiments a 0.5 cm × 0.5 cm grid was printed on the vellum paper, and two strings were used to mark the center of the box in a "T" formation. This ensured the cameras were filming at the correct spot and helped with length scale calibration. Because *A. tonsa* are smaller organisms, the grid interfered with trajectory and swim speed analysis because the image processing system could not distinguish between the *A. tonsa* and the grid. Therefore, plain vellum paper was used without a grid or strings. A calibration stick was used at the start of filming to ensure the cameras were observed the same spot and provide a length scale conversion factor.

Two cameras supported by tripods viewed the T-box apparatus from orthogonal perspectives. Hence, the cameras captured the XZ and YZ perspectives simultaneously. The X and Y coordinates corresponded to the horizontal coordinates of the box (Figure 3.3), and Z was the vertical coordinate. For the *C. finmarchicus* and *T. longicornis* experiments, the cameras were a Pulnix TM 745 (748 × 494 pixels) and a Hitachi KP-M1 ($^2/_3$ inch image chip size with 410,000 pixels). The lenses for these cameras were 60 mm Nikon micro-Nikkor lenses. The images were recorded via JVC VHS VCRs and viewed with Panasonic video monitors. A Horita SMPTE Time Code Generator (TRG-50) simultaneously marked the time on the tapes. The filming was at 30 frames per second (fps). The cameras for the *A. tonsa* experiments were Sony Mini DV Digital Handycams. The resolution was 640 × 480 pixels, and the recording speed was 60 fps. The

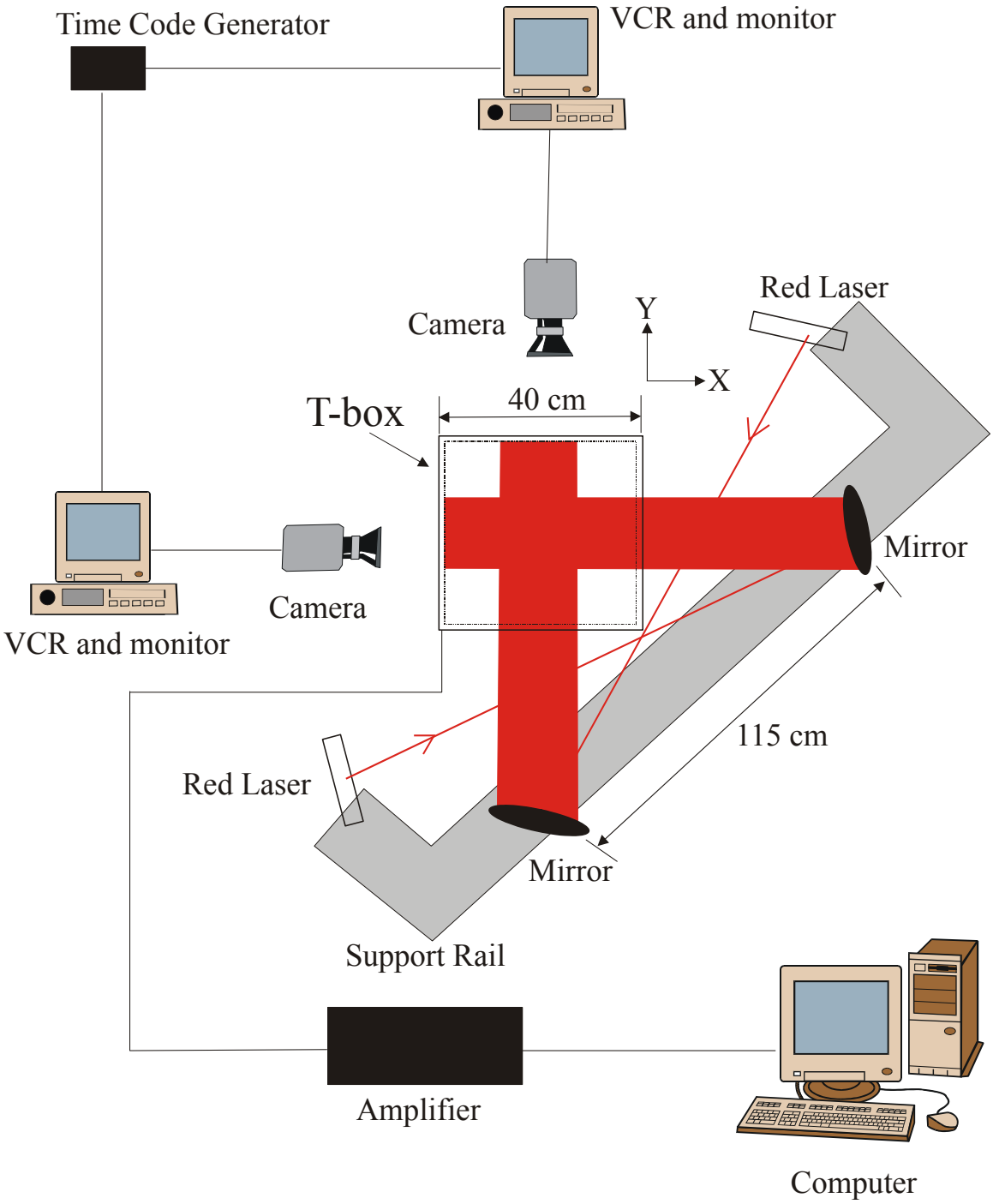

Figure 3.3 Schematic of the experimental set-up during animal behavior observation measurements (top view). Experiments for *Acartia tonsa* employed camcorders rather than the camera/VCR set-up shown.

camcorders for the *A. tonsa* experiment have a viewing window and timer; hence the VCR, monitor system, and time code generator were not needed.

Each experimental test started with T0, the stagnant water condition. Successively higher turbulence intensities were subsequently established in the apparatus. Prior to recording, each turbulence level condition was given sufficient time for the flow to achieve fully isotropic and homogeneous conditions at the box center. Copepod positions are recorded for each T-level for roughly 20 minutes. During the first five minutes there was no green light entering the T-box. At the five minute mark, the green laser was turned on and the beam passed vertically through the center of the box for the remaining 15 minutes.

After changing the turbulence level, there was a wait period of approximately 5 minutes before recording animal behavior. This ensured that the flow conditions were fully established and that copepods were acclimated to the new conditions. Waiting 5-10 minutes also ensured that the copepods escape reaction had equilibrated. Hwang et al. (1994) stated that the copepod *Centropages hamatus* escaped the more frequently during the first 6 minutes of initiated turbulence, and more than 50% of the total escape reactions occurred in this initial period.

The t-test (two-samples assuming unequal variances) was used to statistically compare data within T-levels. The null hypothesis was that there was no difference between the samples. When the test statistic p was less than 0.05, then the null hypothesis was rejected and there was a significant difference between the samples.

A single factor analysis of variance plus the Student Newman-Keuls (SNK) test was performed to statistically compare data sets between T-levels. The SNK test was

performed by ranking the T-level means, determining pairwise difference between the means, and computing a standard error. The test statistic, q, was calculated and compared to $q_{\alpha,\nu,p}$, where α is the significance level, ν is the degrees of freedom within the T-level group, and p is the number of means in the range of means being tested (Zar 1999). The SNK test was used to analyze swimming speed, escape reaction, net-to-gross-displacement ratios, and relative swim speed data sets.

3.4 Copepod Trajectory Analysis

Swimming speed is another valuable tool in understanding copepod behavior. Three-dimensional trajectories were systematically extracted from the video recordings by digitizing the video tapes using ExpertVision software (MotionAnalysis Corp.) at 60 Hz. This program creates text files of all the paths found in the designated image window. The recordings for the XZ and YZ perspectives were digitized separately. The XZ and YZ coordinates of a trajectory are subsequently "matched" to define a fully three-dimensional trajectory. Matches were identified using the TecPlot plotting software package. The XZ and YZ paths were plotted simultaneously on the same axis and a match is declared if the paths have the same time and Z-coordinates. When a match was found, path kinematics were calculated based on the three-dimensional trajectory. For instance, swim speed was calculated by dividing the displacement between sequential frames by the corresponding time delay. As discussed in the next Chapter, the trajectories help to identify behavior patterns and directional preferences of the species.

To demonstrate the convergence of the statistical calculations of the swim speed data, the standard error for each trajectory and each T-level was calculated. The standard

error was calculated as a function of the number of frames included in an individual trajectory. Once the standard error leveled off, the swim speed value had statistically converged. The standard error for the average of all trajectories collected for the same conditions was calculated from the standard deviations of the average swim speed for each of the trajectories.

CHAPTER IV

RESULTS AND DISCUSSION

The behavioral effect of laboratory turbulence on *Acartia tonsa*, *Temora longicornis*, and *Calanus finmarchicus* was analyzed by studying aggregation behavior, trajectory patterns, swim speed, net-to-gross-displacement ratio, and escape reactions. The goal of this analysis is to determine the copepods' behavior changes with different turbulence levels (T-levels): T0, T1, T2, T3, and T4 described in the previous Chapter. The objective of this Chapter is to quantify and discuss the behavioral patterns of the copepods tested.

4.1 Copepod Aggregation to the Light Source

Many copepods are phototactic, which means they can differentiate between light and dark and are often attracted to light (Mauchline 1998). To assess whether copepods could aggregate around a light beam for various turbulence intensity levels, the number of copepods visible on the video monitor per minute was counted for each T-level. The size of the viewing windows for *A. tonsa*, *T. longicornis*, and *C. finmarchicus* were 6 cm × 4.5 cm, 9.5 cm × 7.5 cm, and 12.5 cm × 9.5 cm, respectively. The question to be addressed is whether the copepods can control their movements and continue to phototactically aggregate as the turbulence intensity increases (if they phototactically aggregate in a stagnant environment).

Acartia tonsa is known to be positively phototactic (Stearns and Forward 1984), but Figure 4.1 does not show aggregative behavior to the laser beam. The number in view per minute for light off and light on conditions was similar for each T-level, indicating limited influence of the laser beam. There was a significant difference for light off and light on aggregation for T0 ($p < 0.05$). There were more *A. tonsa* observed for light on conditions than light off, therefore, *A. tonsa* exhibited a phototactic response for stagnant water conditions. The data sets for T1, T2, T3, and T4 light off and light on conditions were statistically coincident. The number in view per minute increased with turbulence level. Again, the increase was likely due to increased mixing and transport of the copepods and hence suggests that they were unable to swim against the velocity fluctuations for the higher turbulence intensity conditions. The flow for higher turbulent intensity conditions tended to transport *A. tonsa* faster, thereby causing a higher number to be in view per minute.

Stearns and Forward (1984) concluded that the light sensitivity of *A. tonsa* is adapted for vertical migration in estuaries. They observed that *A. tonsa* moved toward a directional source of light. In the field, *A. tonsa* exhibit diel migration and peak concentrations occur at dusk and dawn in surface estuarine waters (Buskey et al. 1989). Figure 4.1 does not show a positive phototactic response. This might be because the vertical laser light did not mimic sunlight at the surface of the ocean. *A. tonsa* phototactic behavior also might not be evident from Figure 4.1 because the experiment was conducted in the late morning. *A. tonsa* exhibits a phototactic response over a broad range of wavelengths (380 nm to 700 nm) and is maximally sensitive from ~453 nm to

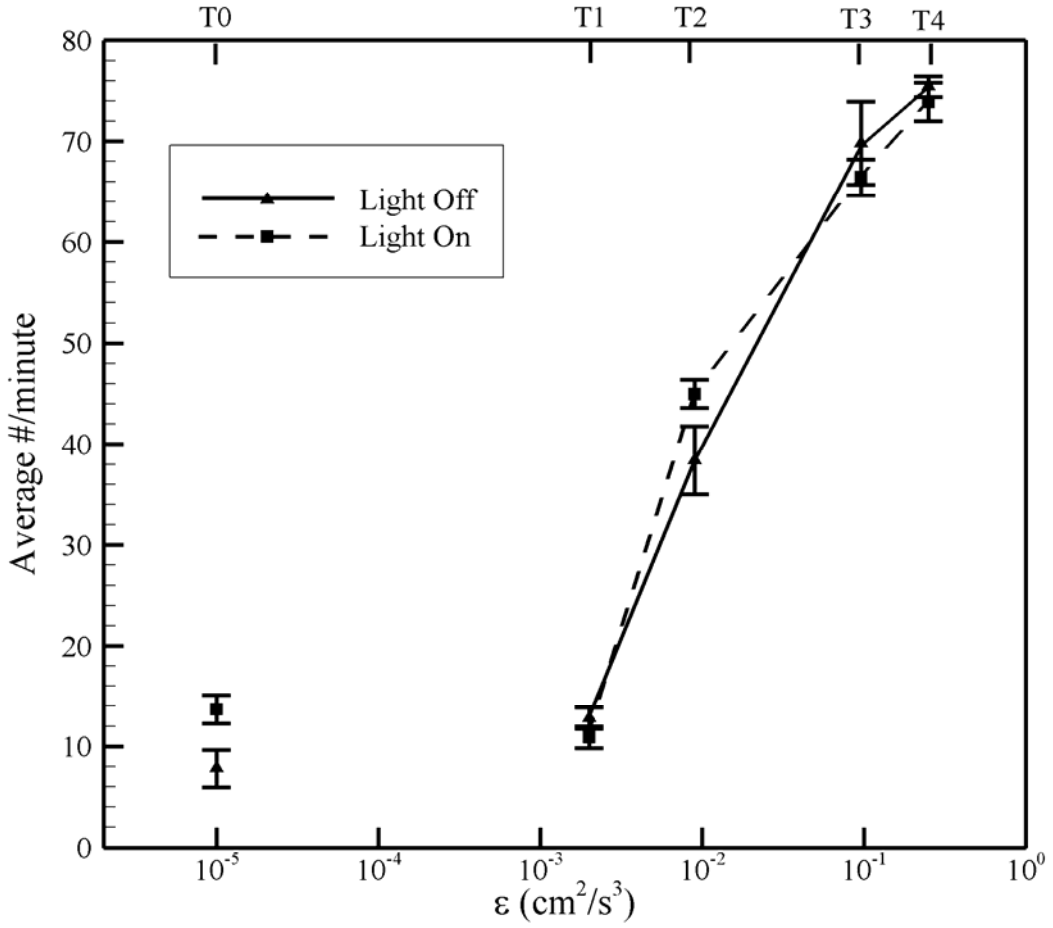

Figure 4.1 Average number of *Acartia tonsa* in field of view per minute for light on and light off conditions.

620 nm (Stearns and Forward 1984). The wavelength of the laser light was 514 nm, which is within the sensitivity range.

Temora longicornis exhibited a positive phototactic response to the light source. For the T0 conditions, the number of copepods in the viewing window without the laser beam projecting through the box was very small. The addition of the light beam increased the number of copepods in the viewing window dramatically ($n = 45$; Figure 4.2). The addition of turbulence increased the number of *T. longicornis* visible on the monitor per minute (Figure 4.2) for the no light conditions. The increase was due to turbulence flow motions advecting the copepods into the field of view. *T. longicornis* aggregated more predominantly to the light source at T0 than at the other T-levels. For T0, the change in number for light off and light on conditions was tested significantly different based on a t-test ($p < 0.001$). *T. longicornis* was unable to exhibit phototactic behavior at higher T-levels. At these turbulence intensities, flow velocities may be greater than their swimming speed. The average number of copepods in view per minute was significantly different for each T-level between light off and light on conditions (t-test, $p < 0.05$).

C. finmarchicus showed little response to the light beam as indicated by the low number of copepods for both light on and light off conditions at T0 (Figure 4.3). The number of *C. finmarchicus* increased slightly for T1 and peaks at T2, with no obvious aggregation due to the light beam presence. The increased number of copepods was due to increased turbulent mixing of the copepods. The number of copepods in the field of view for T3 and T4 was much less than for T2, which suggested that *C. finmarchicus* was able to swim against the flow motion and actively migrate away from the box center,

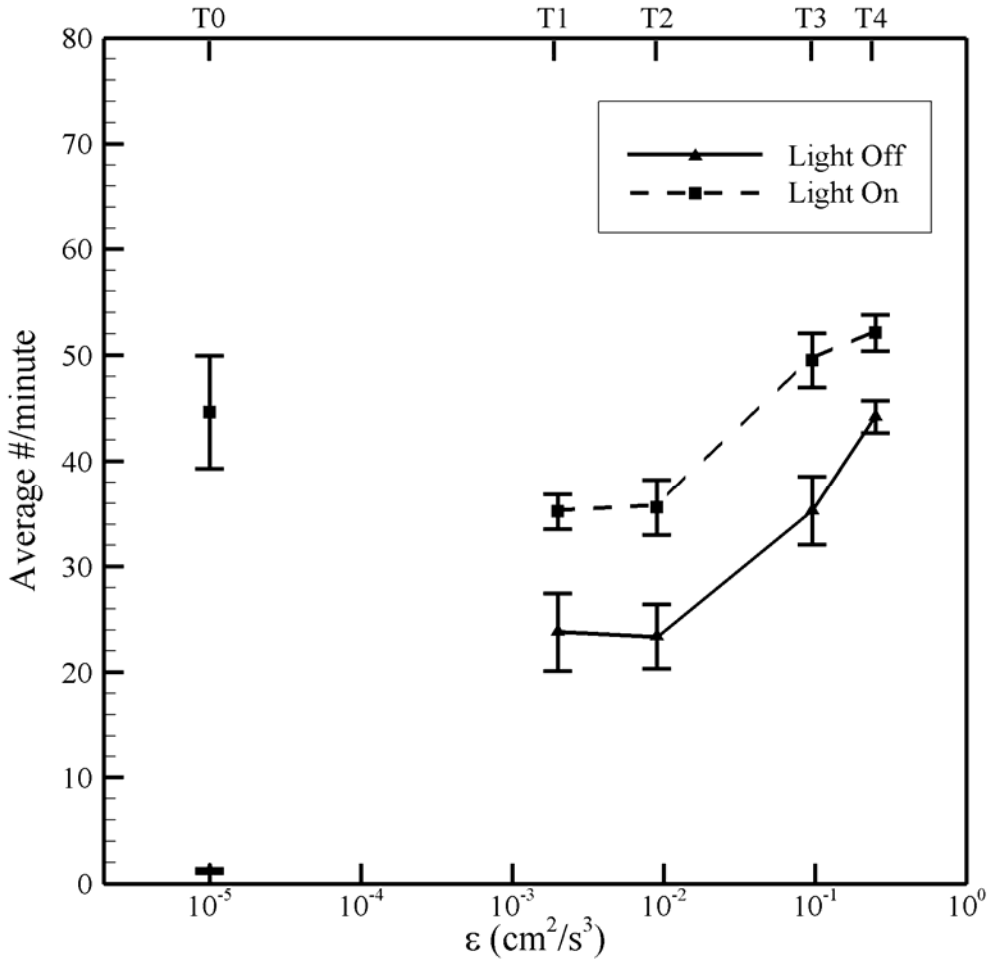

Figure 4.2 Average number of *Temora longicornis* in field of view per minute for light on and light off conditions.

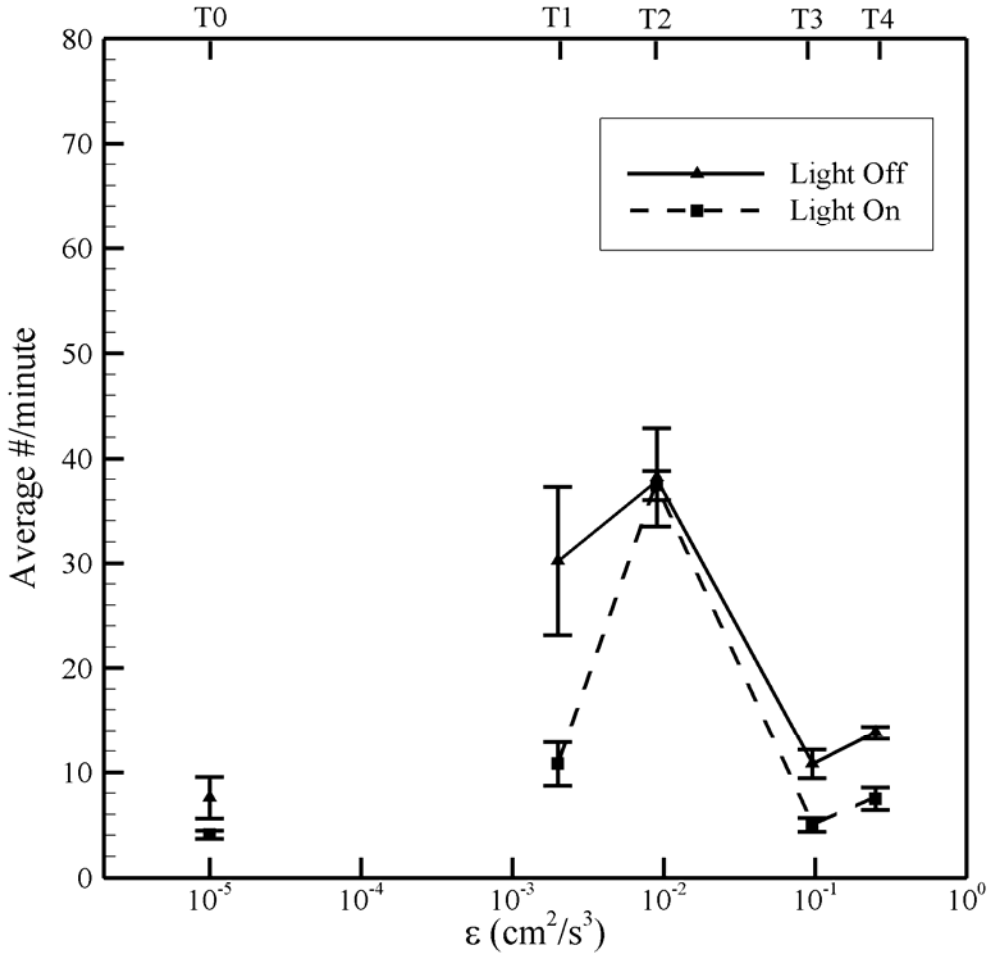

Figure 4.3 Average number of *Calanus finmarchicus* in field of view per minute for light on and light off conditions.

perhaps seeking refuge from turbulence. The potential areas of refuge were near the walls of the T-box because the turbulence intensity is greatly reduced near the solid surface. *C. finmarchicus* exhibited a cruise and sink behavior. T-tests comparing light off and light on aggregation within levels show that T0 and T2 light off and light on conditions were coincident. There was a significant change between light off and light on conditions for T1, T3, and T4 ($p < 0.05$). However, there were more copepods present during light off conditions than light on. This reinforces the observation that C. *finmarchicus* did not exhibit positive phototactic behavior.

Simard et al. (1985) studied the diel migration of *C. finmarchicus*. It was found that *C. finmarchicus* with full stomachs were at deeper depths (30 to 100 m), and the peak concentration of individuals at the surface (0 to 30 m) occurred at dusk and dawn (Simard et al. 1985). *C. finmarchicus* in the T-box experiment may not have shown phototactic behavior for a several reasons. The copepods were fed and the experiment was conducted in the late morning, which was not consistent with the time of day observed for near surface aggregation. The wavelength of the laser light and the vertical orientation of the laser beam also may have influenced the behavior.

Figures 4.1 and 4.2 reveal that *A. tonsa* and *T. longicornis* were more numerous in the field of view for higher T-levels. The faster flow fluctuations tended to transport *A. tonsa* and *T. longicornis* more effectively. Hence, the ability of *T. longicornis* to aggregate to the light source was diminished. *C. finmarchicus*, on the other hand, had the longest bodylength and highest sinking rates (Table 3.2), therefore, it was a larger, heavier animal, and it was not affected by the higher levels of turbulence in the same

manner (Figure 4.3). It is apparent that the size of the copepod is important to discern the swimming ability and behavior of copepods in turbulent flows.

4.2 Swim Speed

Copepod swim speed was calculated from the three-dimensional trajectories measured using the shadowgraph system. The null hypothesis is that the swim speeds are similar between T-levels for *A. tonsa*, *T. longicornis,* and *C. finmarchicus*.

Figures 4.4 to 4.20 are example trajectories for all three species of copepod tested for each T-level. All trajectories begin at the origin (0, 0, 0). The example trajectories were selected randomly and are representative of all trajectories collected for the reported conditions. The *A. tonsa* sample trajectories for T0 to T2 show that *A. tonsa* performed hop and sink motions. The sample trajectories for *C. finmarchicus* show its typical cruising behavior except for the T1 trajectory, which shows an escape and swim pattern (Figure 4.17). The *T. longicornis* sample trajectories demonstrate its cruising behavior except for T0 and T1, which show escape and swim patterns (Figure 4.9 and 4.10).

Swim speed was measured relative to a fixed frame of reference rather than relative to the moving fluid. The measured swim speed peaked at an intermediate turbulence level (Figure 4.21). Measured swim speed is plotted against dissipation rate (ε, cm^2/s^3) and strain rate r. m. s. (σ_{rms}, 1/s). The maximum measured swim speed occurred at T2 (*C. finmarchicus*) or T3 (*A. tonsa* and *T. longicornis*).

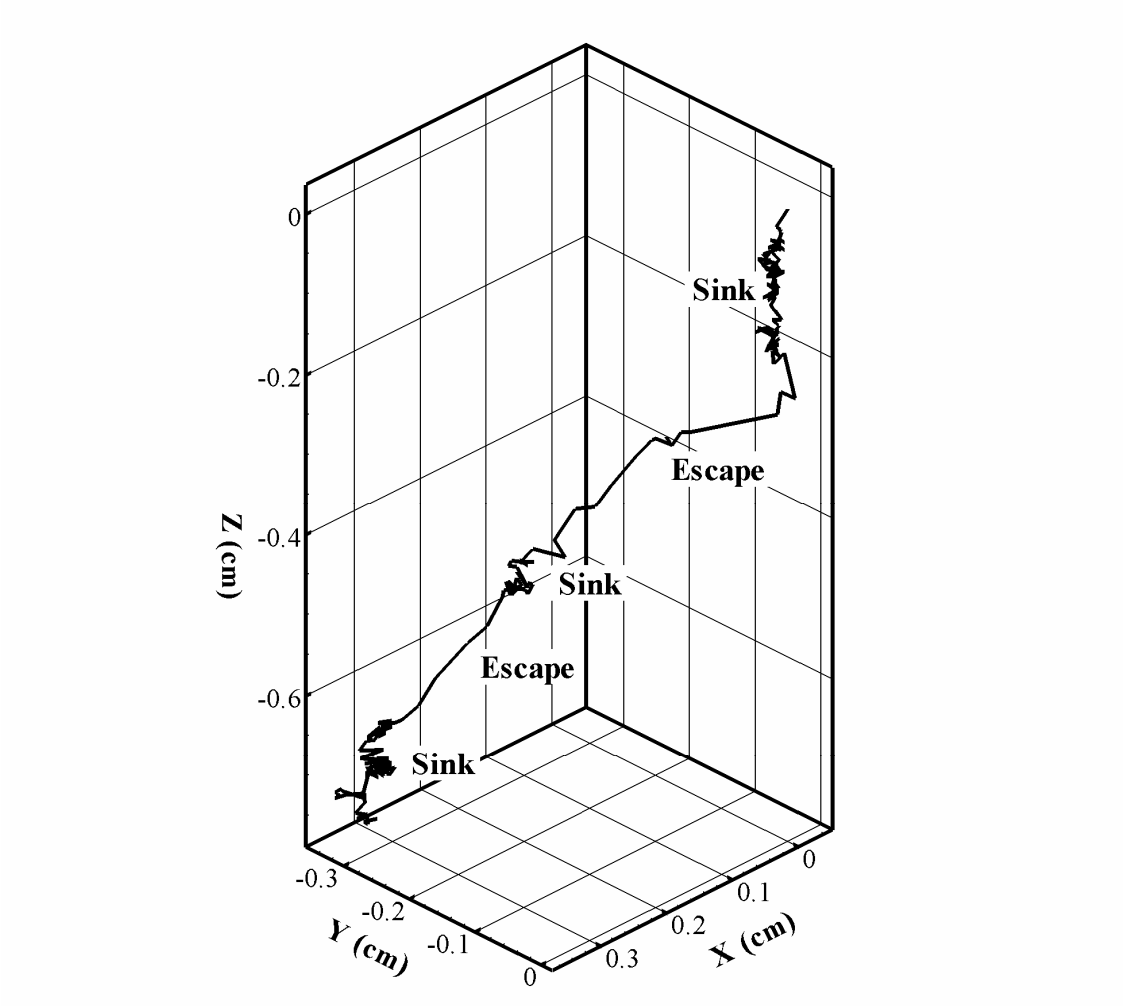

Figure 4.4 Sample *Acartia tonsa* trajectory for T0 including escape and sink patterns. Data extracted at 11:00 of the record.

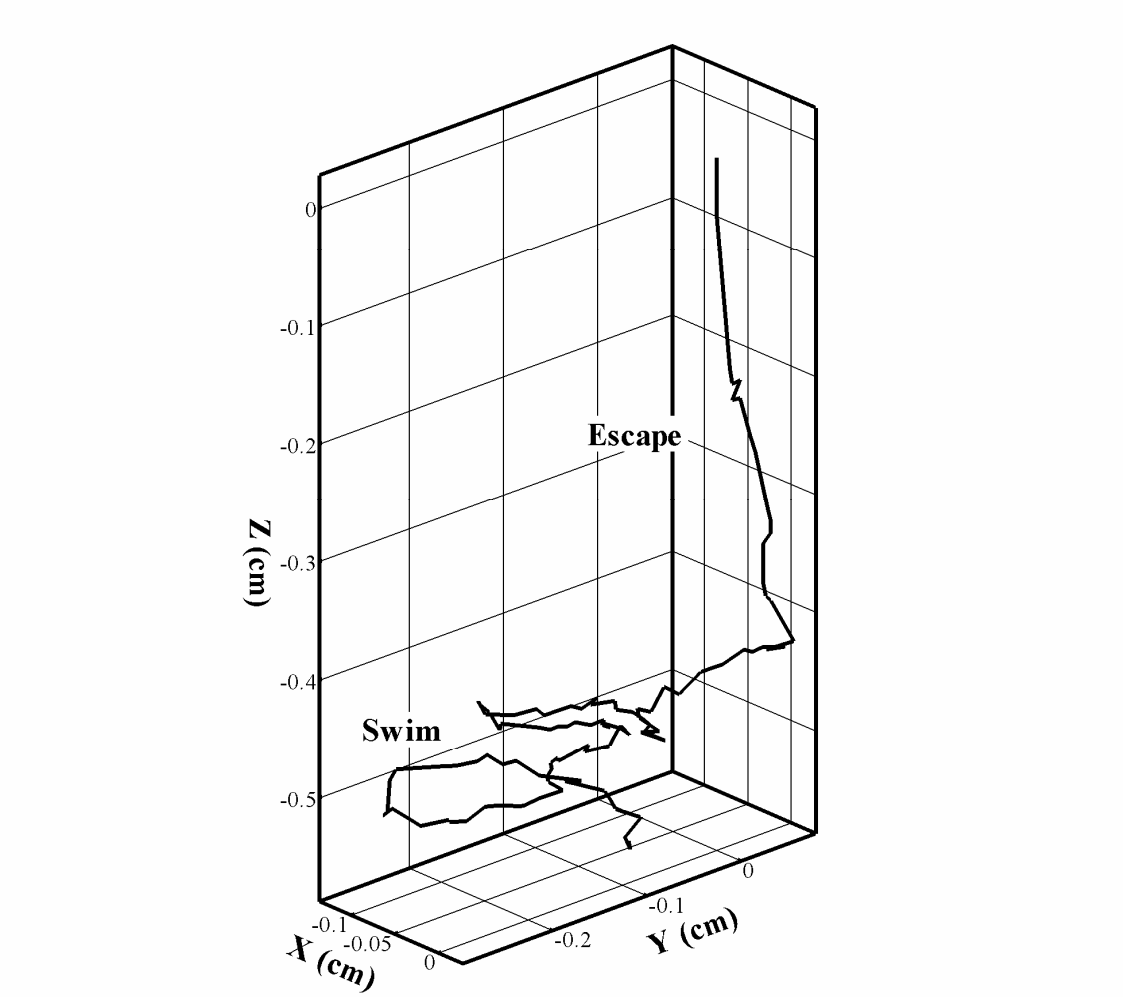

Figure 4.5 Sample *Acartia tonsa* trajectory for T1 including escape and swimming patterns. Data extracted at 13:15 of the record. NGDR is 0.28.

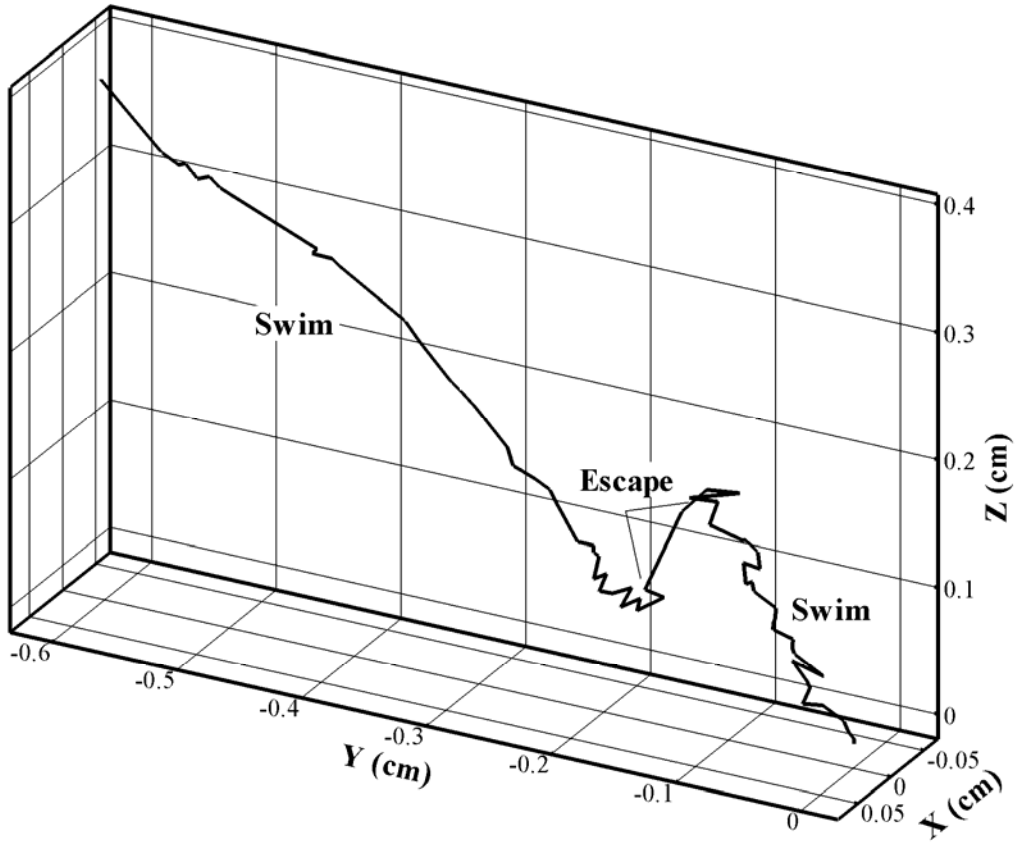

Figure 4.6 Sample *Acartia tonsa* trajectory for T2 including escape and swimming patterns. Data extracted at 16:00 of the record.

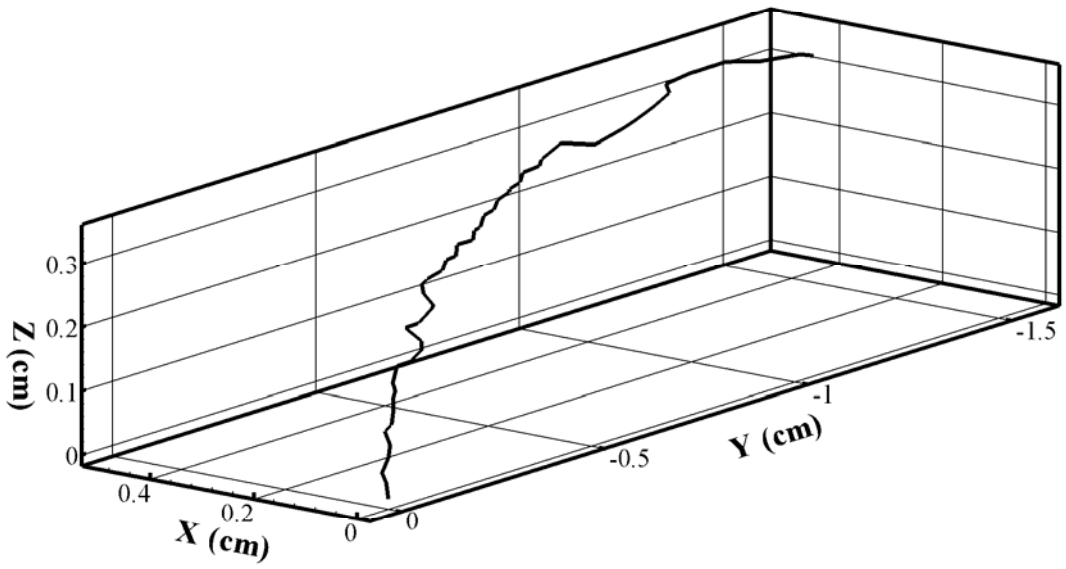

Figure 4.7 Sample *Acartia tonsa* trajectory for T3. Data extracted at 18:00 of the record. NGDR is 0.85.

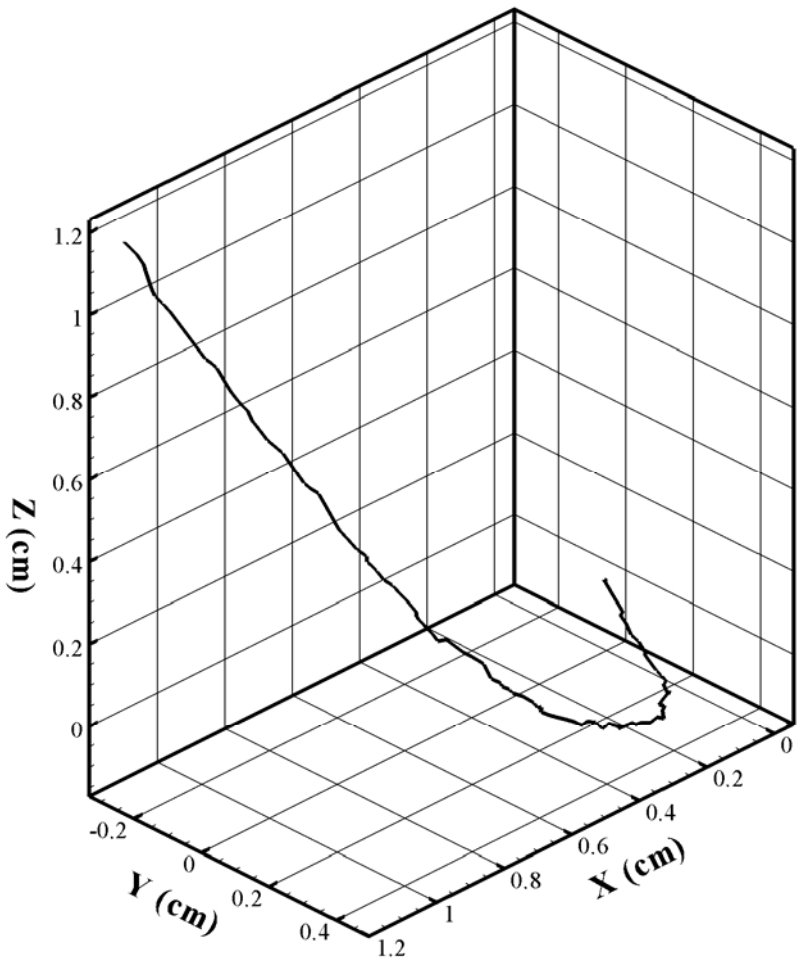

Figure 4.8 Sample *Acartia tonsa* trajectory for T4. Data extracted at 06:15 of the record.

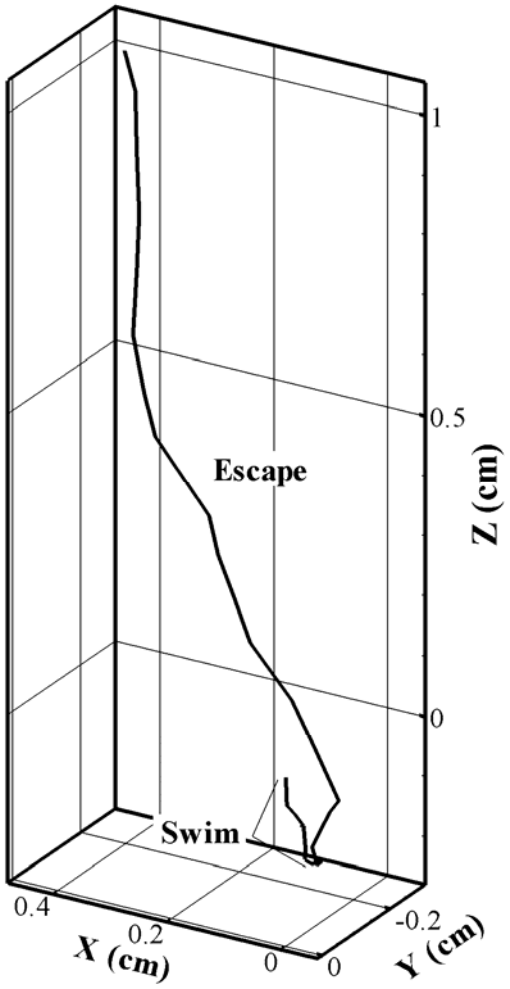

Figure 4.9 Sample *Temora longicornis* trajectory for T0 including escape and swimming patterns. Data extracted at 11:00 of the record.

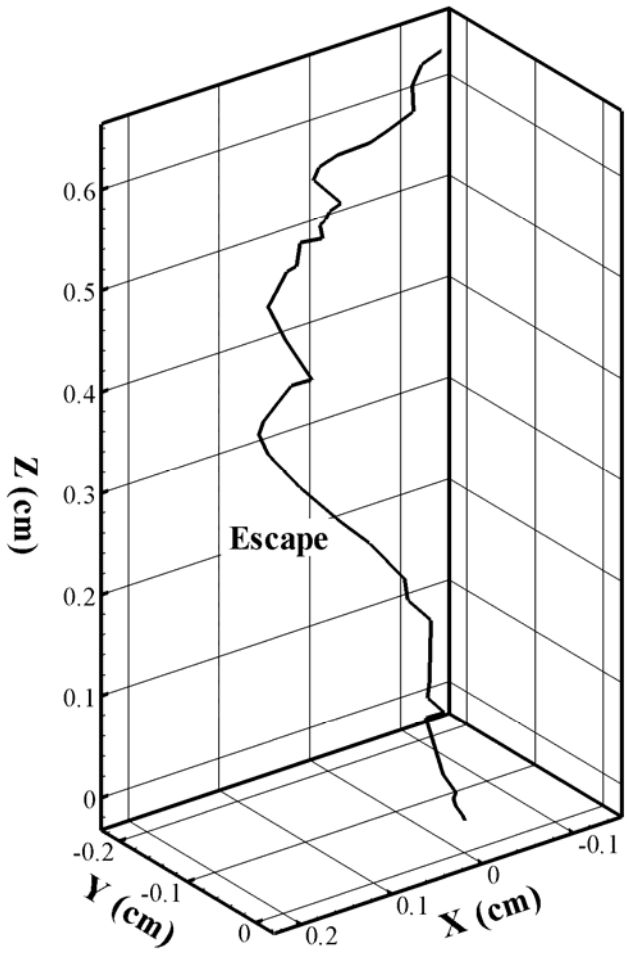

Figure 4.10 Sample *Temora longicornis* trajectory for T1 including an escape pattern. Data extracted at 10:30 of the record.

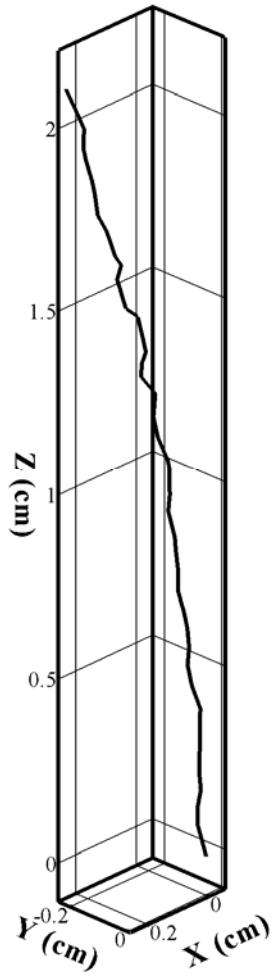

Figure 4.11 Sample *Temora longicornis* trajectory for T1. Data extracted at 12:00 of the record.

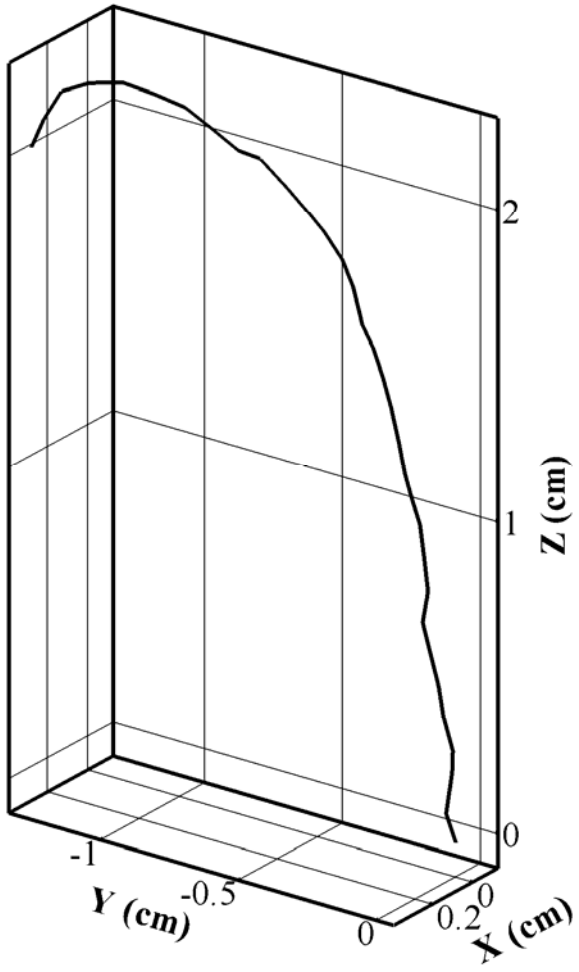

Figure 4.12 Sample *Temora longicornis* trajectory for T1. Data extracted at 15:00 of the record. NGDR is 0.80.

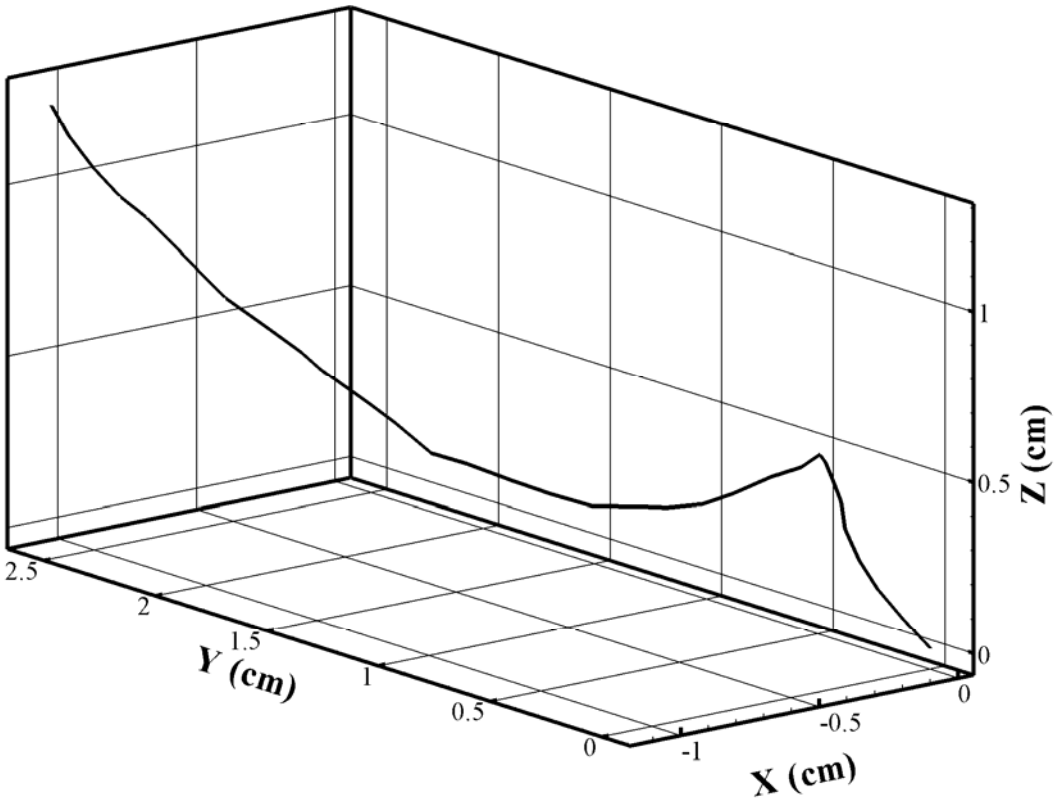

Figure 4.13 Sample *Temora longicornis* trajectory for T2. Data extracted at 15:00 of the record.

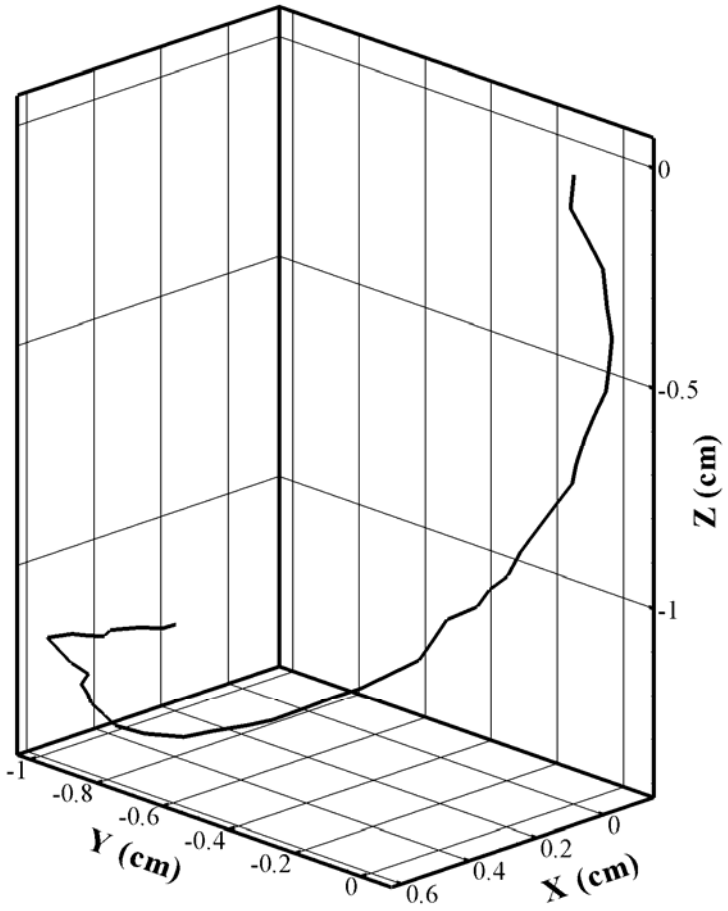

Figure 4.14 Sample *Temora longicornis* trajectory for T3. Data extracted at 13:00 of the record.

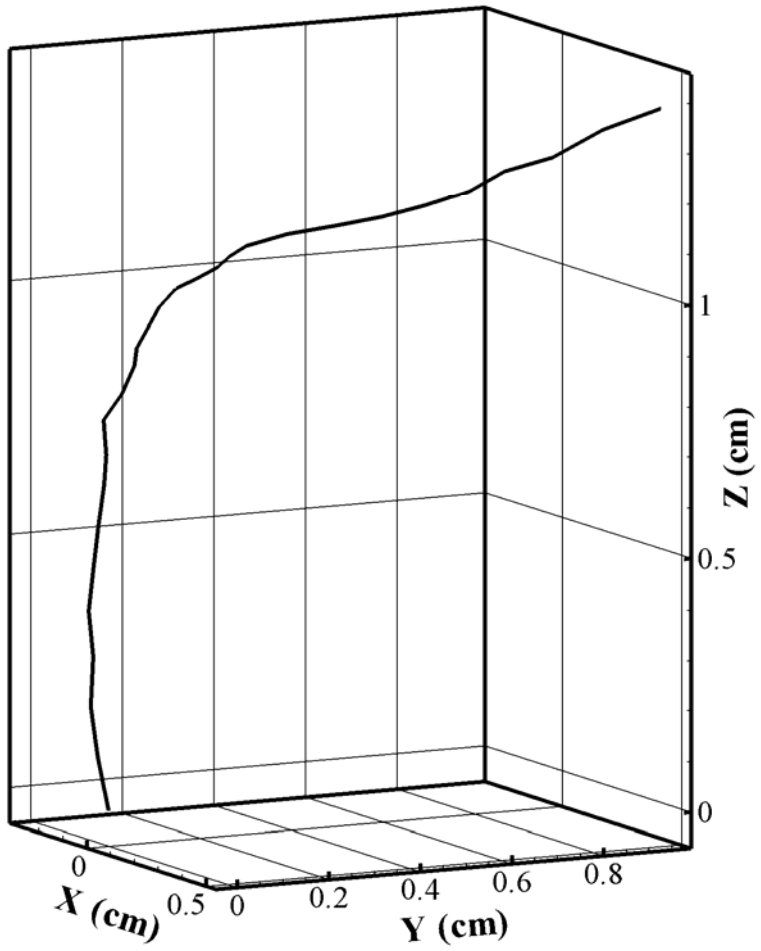

Figure 4.15 Sample *Temora longicornis* trajectory for T4. Data extracted at 05:30 of the record.

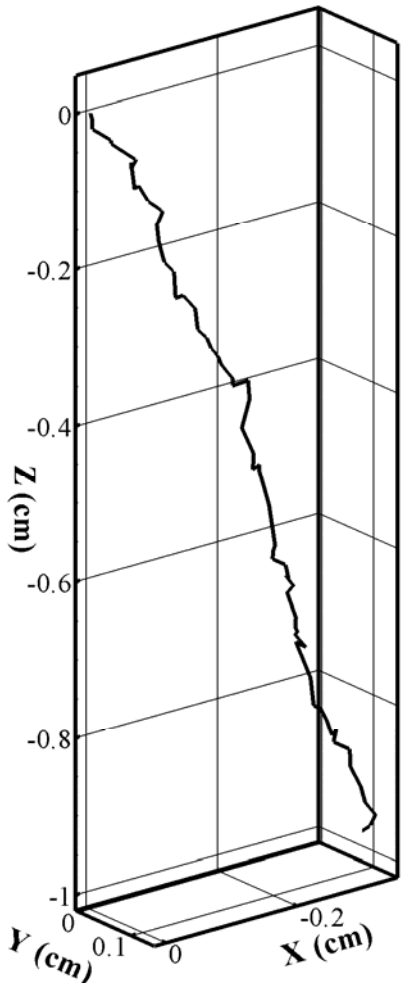

Figure 4.16 Sample *Calanus finmarchicus* trajectory for T0. Data extracted at 02:15 of the record.

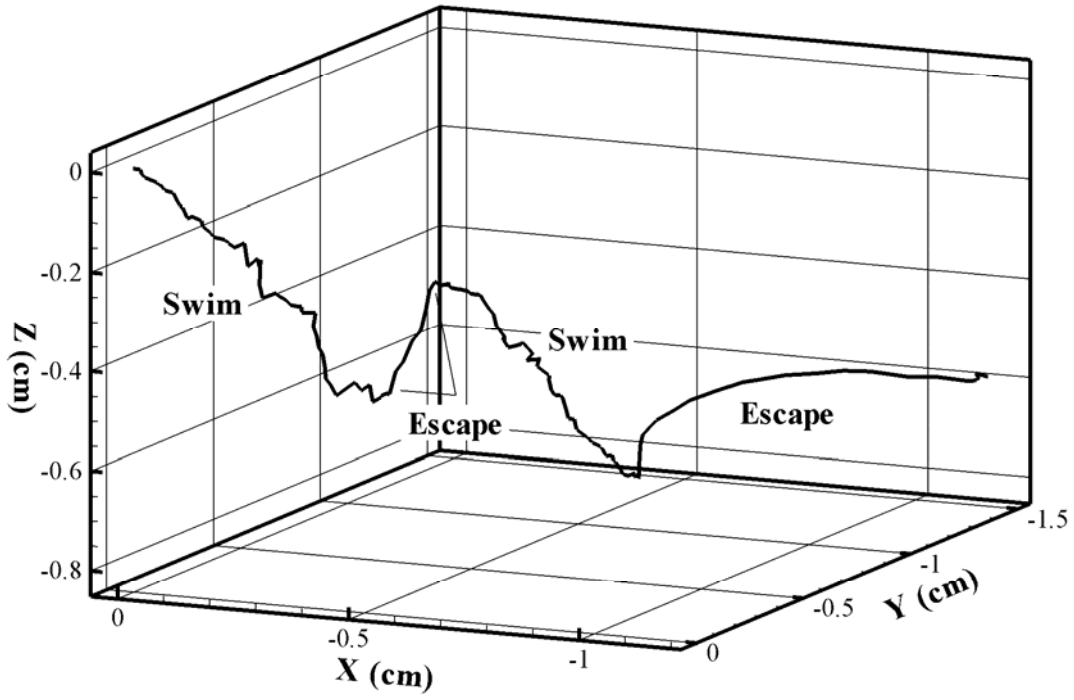

Figure 4.17 Sample *Calanus finmarchicus* trajectory for T1 including escape and swimming patterns. Data extracted at 03:30 of the record.

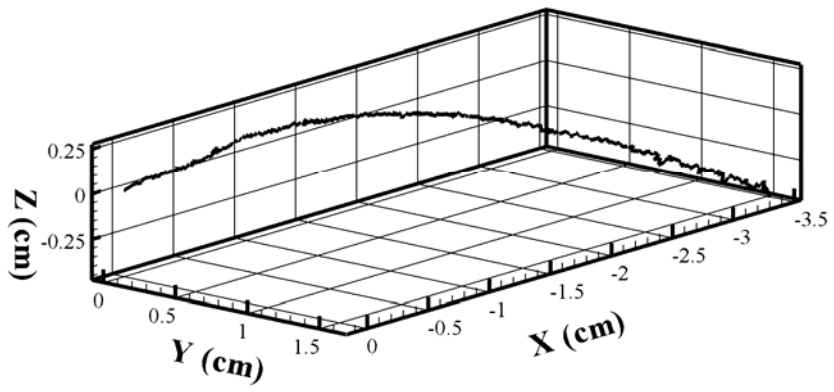

Figure 4.18 Sample *Calanus finarchicus* trajectory for T2. Data extracted at 14:00 of the record.

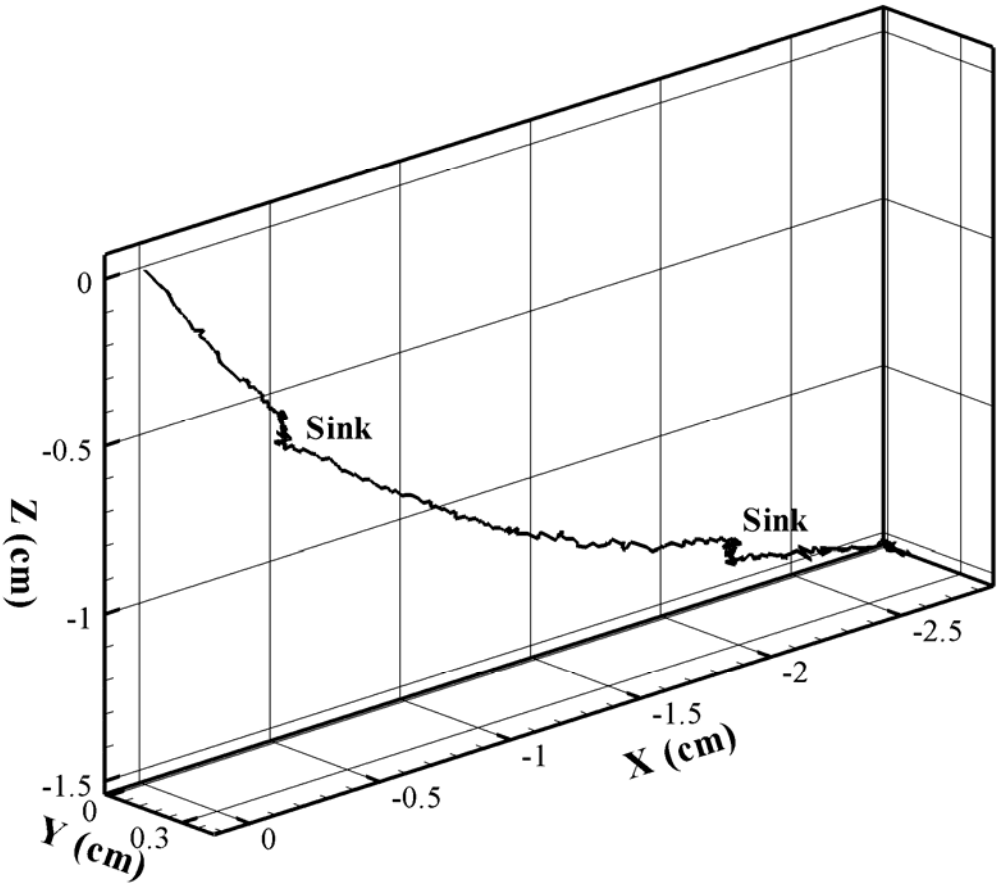

Figure 4.19 Sample *Calanus finmarchicus* trajectory for T3 including sinking patterns. Data extracted from minute 09:00 of the record.

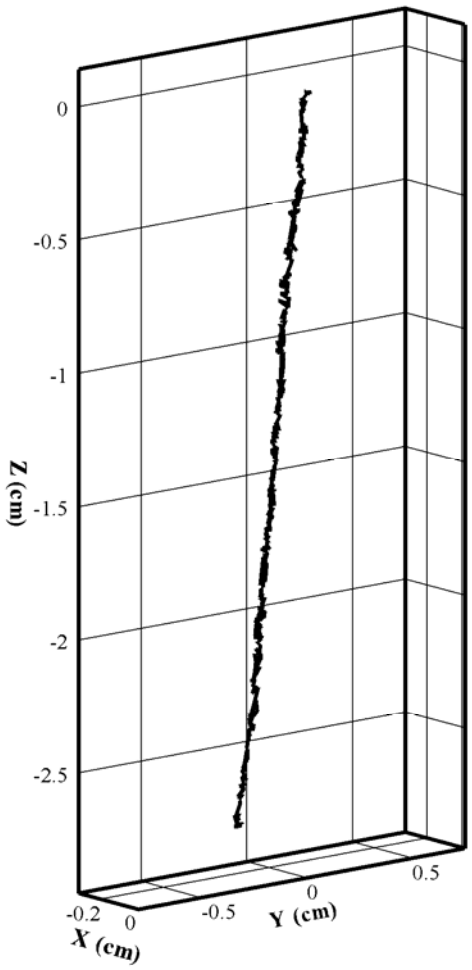

Figure 4.20 Sample *Calanus finmarchicus* trajectory for T4. Data extracted at 10:30 of the record.

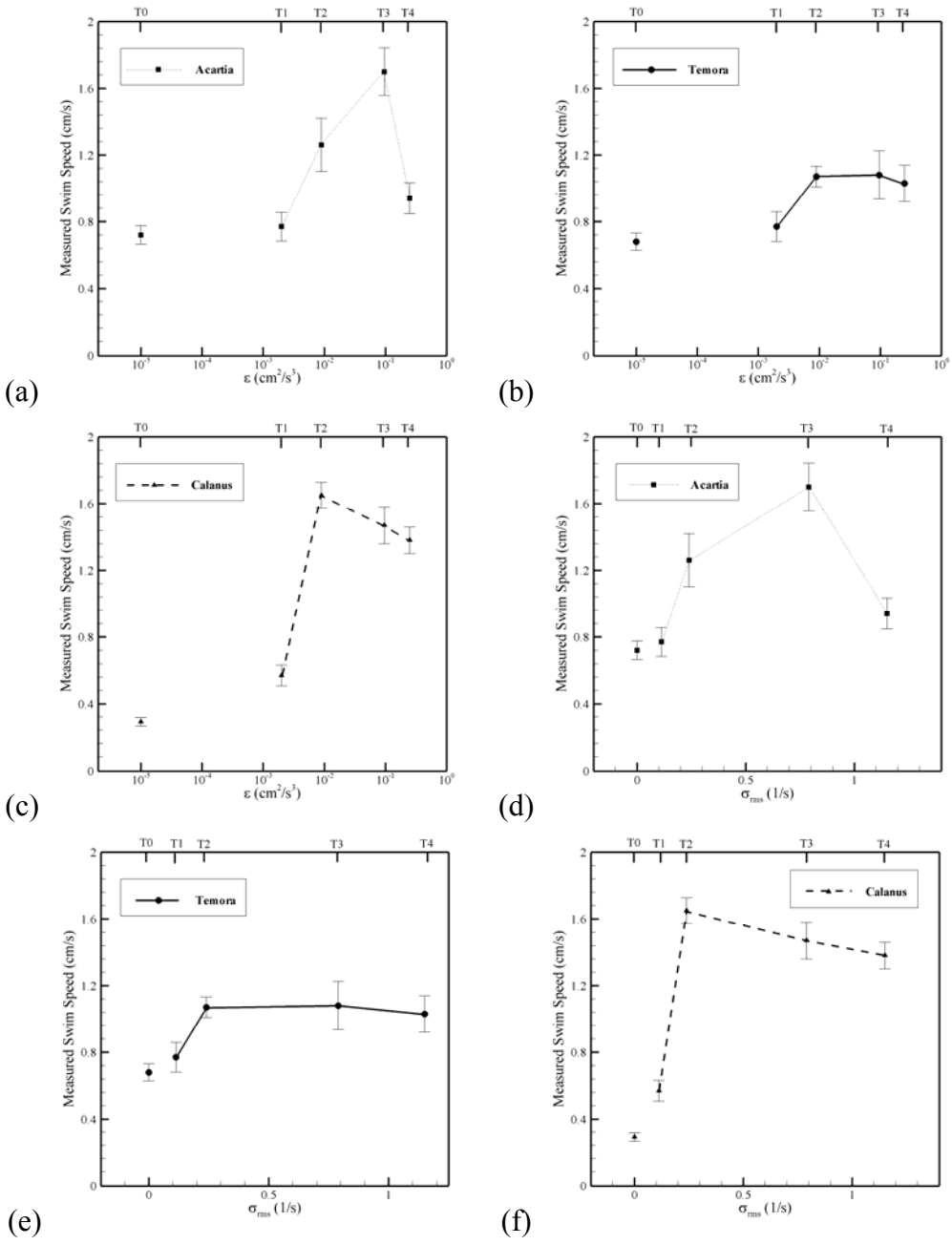

Figure 4.21 Measured swim speed for (a), (b) *Acartia tonsa*, (c), (d) *Temora longicornis*, and (e), (f) *Calanus finmarchicus* as a function of turbulence intensity

The standard deviation of swim speed (i.e. the square root of the variance around the mean reported in Figure 4.21) was calculated for each species as a function of turbulence (Figure 4.22). Standard deviation is plotted against dissipation rate (ε, cm^2/s^3) and strain rate r. m. s. (σ_{rms}, 1/s). The standard deviation was calculated for each trajectory, and the reported data are the average of all trajectories for each T-level. *C. finmarchicus* and *A. tonsa* swim speed standard deviation peak at T3 (1.04 cm/s and 0.88 cm/s respectively). *C. finmarchicus* shows the greatest range of variability of the three species. Table 4.1 shows the results of the Student Newman-Keuls test for standard deviation of swim speed. Pairwise comparisons were made between T-levels for each of the three species. A rejection of the test means that there was a significant difference in data sets between the corresponding T-levels. An acceptance of the test means there was not enough evidence to conclude the data sets were different. There were no significant differences for any of the pairwise comparisons for *A. tonsa* and *T. longicornis* for standard deviation of swim speed. It may be assumed these data sets were statistically coincident. Swim speed fluctuation for *C. finmarchicus* was significantly higher at T2, T3, and T4 compared to that at T0 and T1.

The relative swim speed equals the measured swim speed minus the root mean squared (r.m.s.) velocity for the turbulent flow fields. The r.m.s. velocity is representative of the intensity of the fluid velocity for each turbulence level. It is not, however, representative of the instantaneous fluid velocity surrounding the copepod. Thus, the relative swim speed reported here is a statistical representation of the average movement of the copepod compared to the average strength of the fluid velocity fluctuations. For all three species, the relative swim speed increased from T0 to T2 then

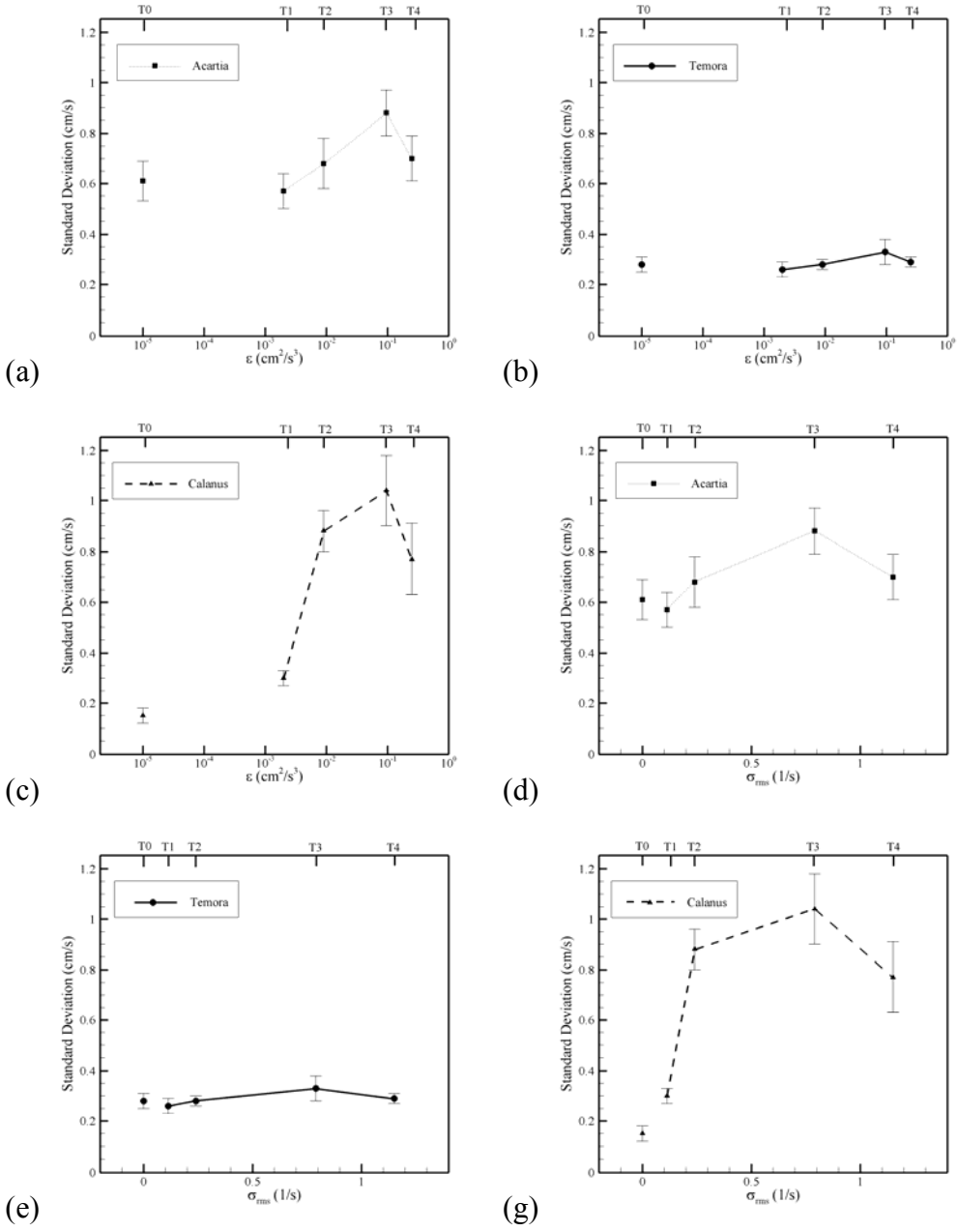

Figure 4.22 Standard deviation of swim speed for (a), (b) *Acartia tonsa*, (c), (d) *Temora longicornis*, and (e), (f) *Calanus finmarchicus* as a function of turbulence intensity.

Table 4.1 Results of Student Newman-Keuls test for standard deviation of swim speed. Rejection indicates a significant difference, whereas acceptance indicates there is not enough evidence to conclude the data sets are different.

(a) *A. tonsa*

Comparison	q	$q_{0.05,\nu,p}$	Conclusion
T3 v. T1	3.26	4.04	Accept
T3 v. T0	3.31	3.79	Accept
T3 v. T2	2.07	3.44	Accept
T3 v. T4	2.26	3.86	Accept
T4 v. T1	1.38	4.04	Accept
T4 v. T0	1.14	3.79	Accept
T4 v. T2	0.25	3.44	Accept
T2 v. T1	0.95	4.04	Accept
T2 v. T0	0.68	3.79	Accept
T0 v. T1	0.38	4.04	Accept

(b) *T. longicornis*

T3 v. T1	1.91	4.04	Accept
T3 v. T0	1.37	3.79	Accept
T3 v. T2	1.34	3.44	Accept
T3 v. T4	0.99	3.86	Accept
T4 v. T1	0.99	4.04	Accept
T4 v. T0	0.43	3.79	Accept
T4 v. T2	0.30	3.44	Accept
T2 v. T1	0.78	4.04	Accept
T2 v. T0	0.17	3.79	Accept
T0 v. T1	0.55	4.04	Accept

(c) *C. finmarchicus*

T3 v. T0	8.54	4.039	Reject
T3 v. T1	9.51	3.791	Reject
T3 v. T4	1.99	3.442	Accept
T3 v. T2	1.92	3.858	Accept
T2 v. T0	7.82	4.039	Reject
T3 v. T1	9.18	3.791	Reject
T2 v. T4	0.90	3.442	Accept
T4 v. T0	4.39	4.039	Reject
T4 v. T1	3.80	3.791	Reject
T1 v. T0	1.63	4.039	Accept

decreased from T2 to T4 (Figure 4.23). The maximum relative swim speed for each species occurred at T2. The relative swim speeds for *A. tonsa*, *T. longicornis*, and *C. finmarchicus* at T0 and T2 were 0.72, 0.68, 0.29 cm/s and 0.98, 0.79, 1.4 cm/s, respectively. Thus, it can be concluded that the organisms were able to overcome the velocity of the flow field for T0, T1, and T2; however, for T3 and T4 the copepods were transported by the flow field rather than swimming (Figure 4.23). *T. longicornis* and *A. tonsa* were barely able to overcome the flow velocity in T4.

The motility number (Mn) was calculated to determine if copepod swimming overcomes the physical flow field at the four T-levels. The Mn is defined as the ratio of measured copepod swimming speed and the r.m.s. turbulent velocity (Gallager et al. 2004). Gallager et al. (2004) observed that copepods in the ocean could aggregate for Mn greater than three, whereas they did not aggregate when Mn was smaller. Thus, if Mn is greater than three, then plankton behavior dominates over the physical forcing, i.e. the copepod can swim through the flow field. In the current data, Mn for T1 and T2 was greater than three, and Mn was less than three for T3 and T4 (Figure 4.24). The Mn for T0 was not calculated, because the flow r.m.s. velocity value is zero. Therefore, the conclusion drawn from the Mn is the same as that concluded from other parameters. For T1 and T2, copepod swimming behavior dominated over the physical flow, whereas for T3 and T4 the physical transport of the fluid dominated. The Mn for *A. tonsa*, *T. longicornis*, and *C. finmarchicus* for T1 and T2 are significantly higher than the Mn for T3 and T4 (see Table 4.2 for Student Newman-Keuls test results). This reemphasizes the fact that as the turbulence increases, the copepod's behavior becomes dominated by the physical flow.

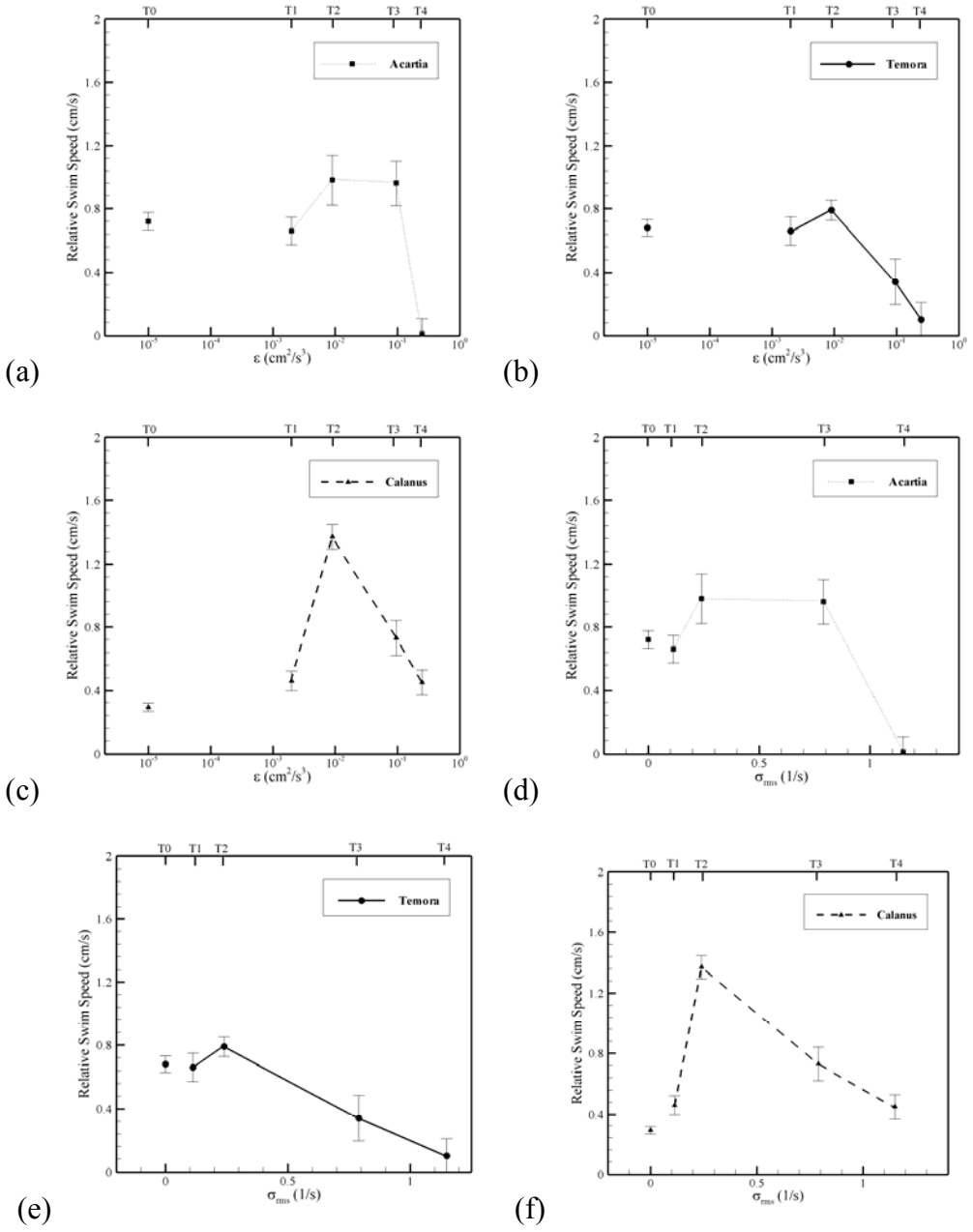

Figure 4.23 Relative swim speed for (a), (b) *Acartia tonsa*, (c), (d) *Temora longicornis*, and (e), (f) *Calanus finmarchicus* as a function of turbulence intensity.

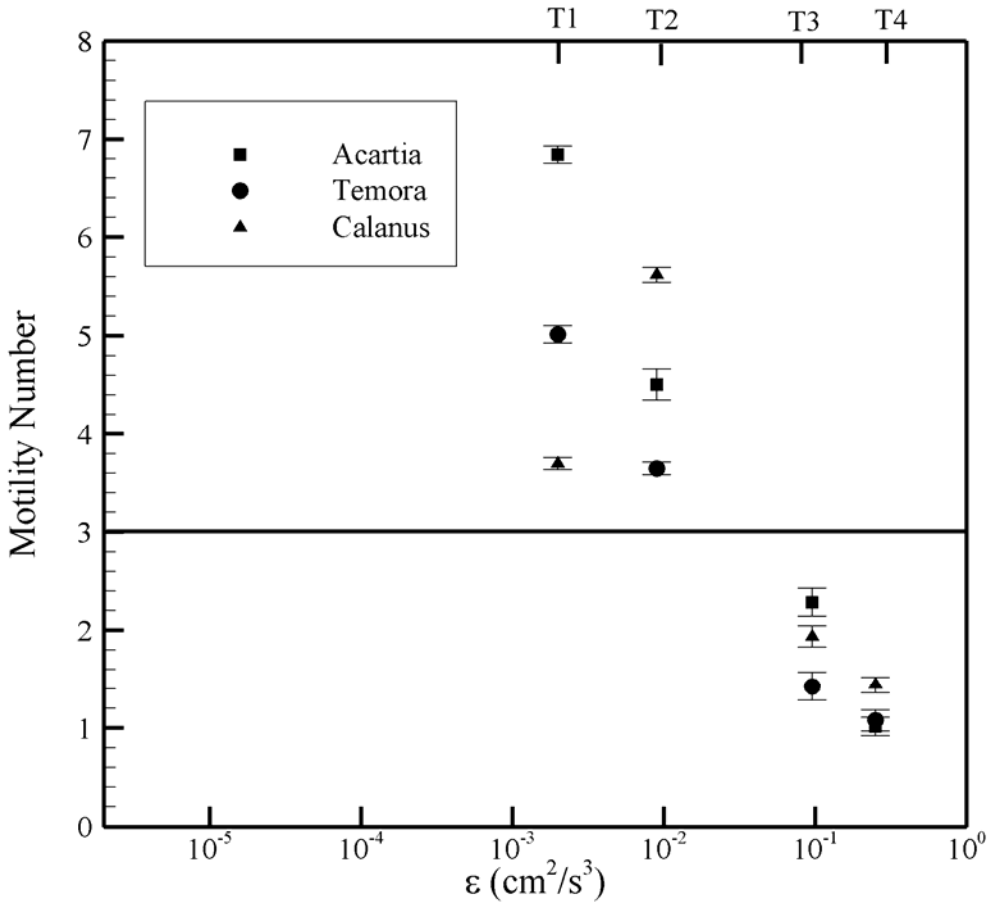

Figure 4.24 Motility number (measured swim speed divided by r.m.s. of the flow velocity) for *A. tonsa*, *T. longicornis*, and *C. finmarchicus* as a function of turbulence intensity. Data points above the horizontal line at *Mn* 3 indicate that copepod swimming dominates over physical transport (Gallager et al. 2004).

Table 4.2 Results of Student Newman-Keuls test for motility number (Mn). Rejection indicates a significant difference, whereas acceptance indicates there is not enough evidence to conclude the data sets are different.

(a) *A. tonsa*

Comparison	q	$q_{0.05,\nu,p}$	Conclusion
T1 v. T4	15.8	3.79	Reject
T1 v. T3	12.2	3.44	Reject
T1 v. T2	5.35	3.86	Reject
T2 v. T4	9.01	3.79	Reject
T2 v. T3	5.68	3.44	Reject
T3 v. T4	4.03	3.79	Reject

(b) *T. longicornis*

T1 v. T4	13.5	3.74	Reject
T1 v. T3	11.7	3.40	Reject
T1 v. T2	7.77	2.83	Reject
T2 v. T4	6.96	3.74	Reject
T2 v. T3	5.51	3.40	Reject
T3 v. T4	0.75	3.74	Accept

(c) *C. finmarchicus*

T2 v. T4	5.65	3.791	Reject
T2 v. T3	7.99	3.442	Reject
T2 v. T1	2.12	3.858	Accept
T1 v. T4	4.60	3.791	Reject
T1 v. T3	6.38	3.442	Reject
T3 v. T4	0.59	3.791	Accept

Standard error was calculated for each trajectory as a function of the number of frames. When standard error leveled off, the swim speed values had statistically converged. Figure 4.25 is an example standard error trend for an *A. tonsa* trajectory. Standard error was calculated for each T-level as a function of the number of trajectories. Figure 4.26 is an example standard error trend as a function of the number of trajectories for *T. longicornis* at T2.

Table 4.3 shows the results of the Student Newman-Keuls test for relative swim speed. The relative swim speed for *A. tonsa* at T4 was significantly different from the other T-levels, which were statistically coincident. The *A. tonsa* relative swim speed at T4 was 0.01 cm/s, which means the swim speed was approximately equal to the r.m.s. fluid velocity for T4. The relative swim speed for *C. finmarchicus* at T2 was significantly different from the other T-levels, which were statistically coincident. The shape of the *C. finmarchicus* relative swim speed plot resembles a dome. *T. longicornis* relative swim speed for T0, T1, and T2 were statistically coincident, while there was a significant decrease for T3 and T4.

The size of the species directly relates to the relative swim speed. The largest species, *C. finmarchicus*, had the highest relative swim speed (0.45 cm/s) at T4. *C. finmarchicus* was stronger and better equipped (by size) to overcome the flow field. The smallest species, *A. tonsa*, had the smallest relative velocity for T4. Hence, we conclude that *A. tonsa* did not have the power to overcome the turbulent flow field.

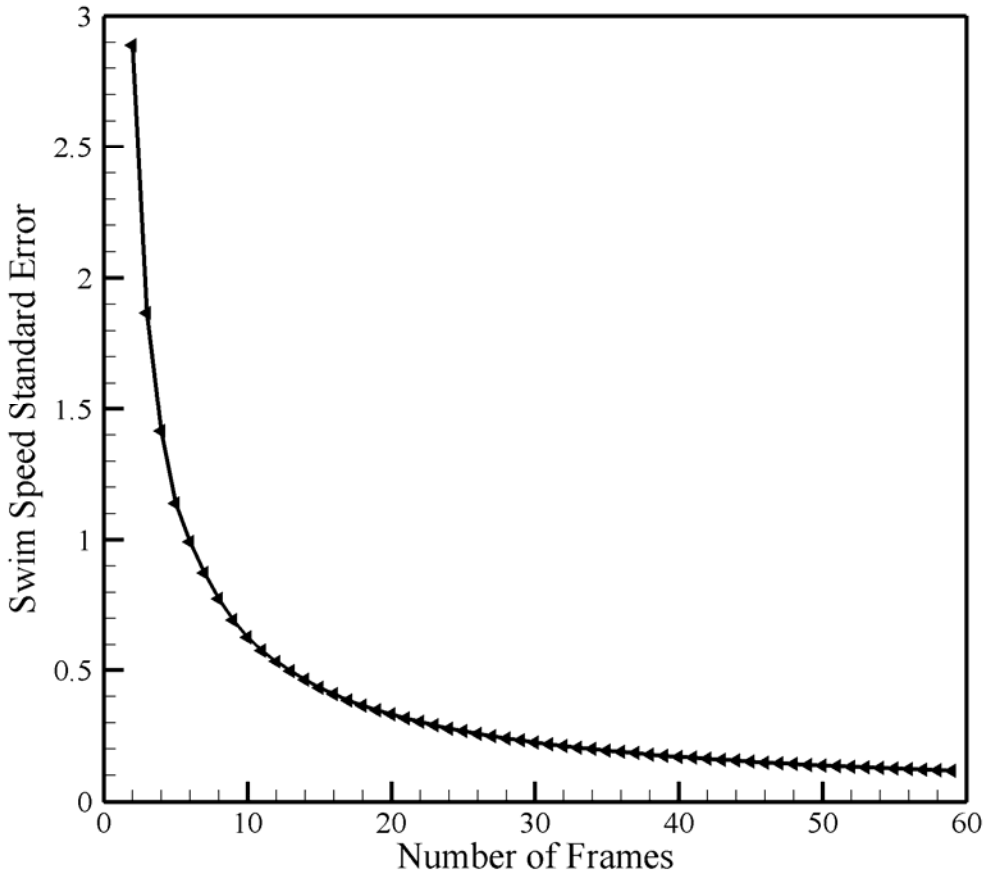

Figure 4.25 Standard error of swim speed data as a function of the number of frames for an example *Acartia tonsa* trajectory for T1.

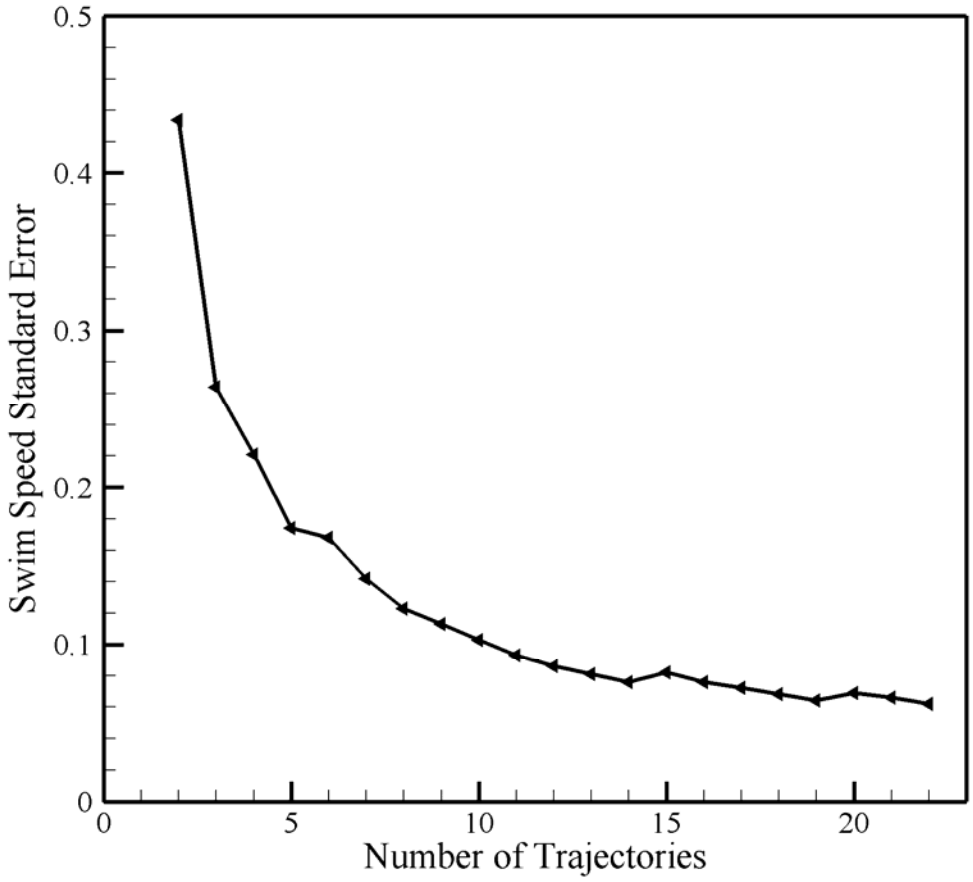

Figure 4.26 Standard error of swim speed data as a function of the number of trajectories for *Temora longicornis* for T2.

Table 4.3 Results of Student Newman-Keuls test for relative swim speed. Rejection indicates a significant difference, whereas acceptance indicates there is not enough evidence to conclude the data sets are different.

(a) *A. tonsa*

Comparison	q	$q_{0.05,\nu,p}$	Conclusion
T2 v. T4	8.21	4.04	Reject
T2 v. T1	2.62	3.79	Accept
T2 v. T0	2.40	3.44	Accept
T2 v. T3	0.91	3.86	Accept
T3 v. T4	8.98	4.04	Reject
T3 v. T1	2.10	3.79	Accept
T3 v. T0	1.82	3.44	Accept
T0 v. T4	6.96	4.04	Reject
T0 v. T1	0.52	3.79	Accept
T1 v. T4	5.49	4.04	Reject

(b) *T. longicornis*

T2 v. T4	8.37	3.98	Reject
T2 v. T3	4.99	3.74	Reject
T2 v. T1	1.60	3.40	Accept
T2 v. T0	1.35	2.83	Accept
T0 v. T4	6.30	3.98	Reject
T0 v. T3	3.43	3.74	Accept
T0 v. T1	0.20	3.40	Accept
T1 v. T4	6.21	3.98	Reject
T1 v. T3	3.29	3.74	Accept
T3 v. T4	2.42	3.98	Accept

(c) *C. finmarchicus*

T2 v. T0	10.9	4.04	Reject
T2 v. T4	7.03	3.79	Reject
T2 v. T1	13.7	3.44	Reject
T2 v. T3	7.84	3.86	Reject
T3 v. T0	3.99	4.04	Accept
T3 v. T4	1.98	3.79	Accept
T3 v. T1	3.32	3.44	Accept
T1 v. T0	1.70	4.04	Accept
T1 v. T4	0.05	3.79	Accept
T4 v. T0	1.07	4.04	Accept

Typical swim speeds for all three species are presented in Table 3.2. The reported typical swim speed for *A. tonsa* ranges from 1-8 mm/s. In the current experiments, the lowest relative swim speed for *A. tonsa* was 0.01 cm/s (0.1 mm/s) for T4, and the highest was 0.98 cm/s (9.8 mm/s) at T2 (Figure 4.23). The reported typical swim speed for *C. finmarchicus* ranges from 2-5 mm/s with a maximum of 10 mm/s. The range of relative swim speeds was 0.29-1.4 cm/s (2.9-14 mm/s) (Figure 4.23). The reported typical swim speed for *T. longicornis* ranges from 2.7-6.1 mm/s. The range of relative swim speeds was 0.10-0.79 cm/s (1.0-7.9 mm/s) (Figure 4.23). Thus, the relative swim speed for all three species in turbulent flow lies within or close to the reported typical ranges (Buskey and Swift 1985, Buskey et al. 1986, Buskey 1994, Hirche 1987, and Tiselius 1992).

4.3 Net to Gross Displacement Ratio

Net-to-gross-displacement ratio (NGDR) measures the tortuousity of the organism's path. NGDR ranges from zero to one, zero being the most tortuous path to one being the least tortuous (straightest) path. The question to be answered is how the trajectories change for *A. tonsa*, *T. longicornis*, and *C. finmarchicus* with increasing turbulence.

The NGDR presented in Figure 4.27 is the average of all trajectories for each T-level. The net displacement was calculated by finding the distance between the final point and the initial point. The gross displacement was the sum of the distances between all intermediate points (i.e. the length of the path).

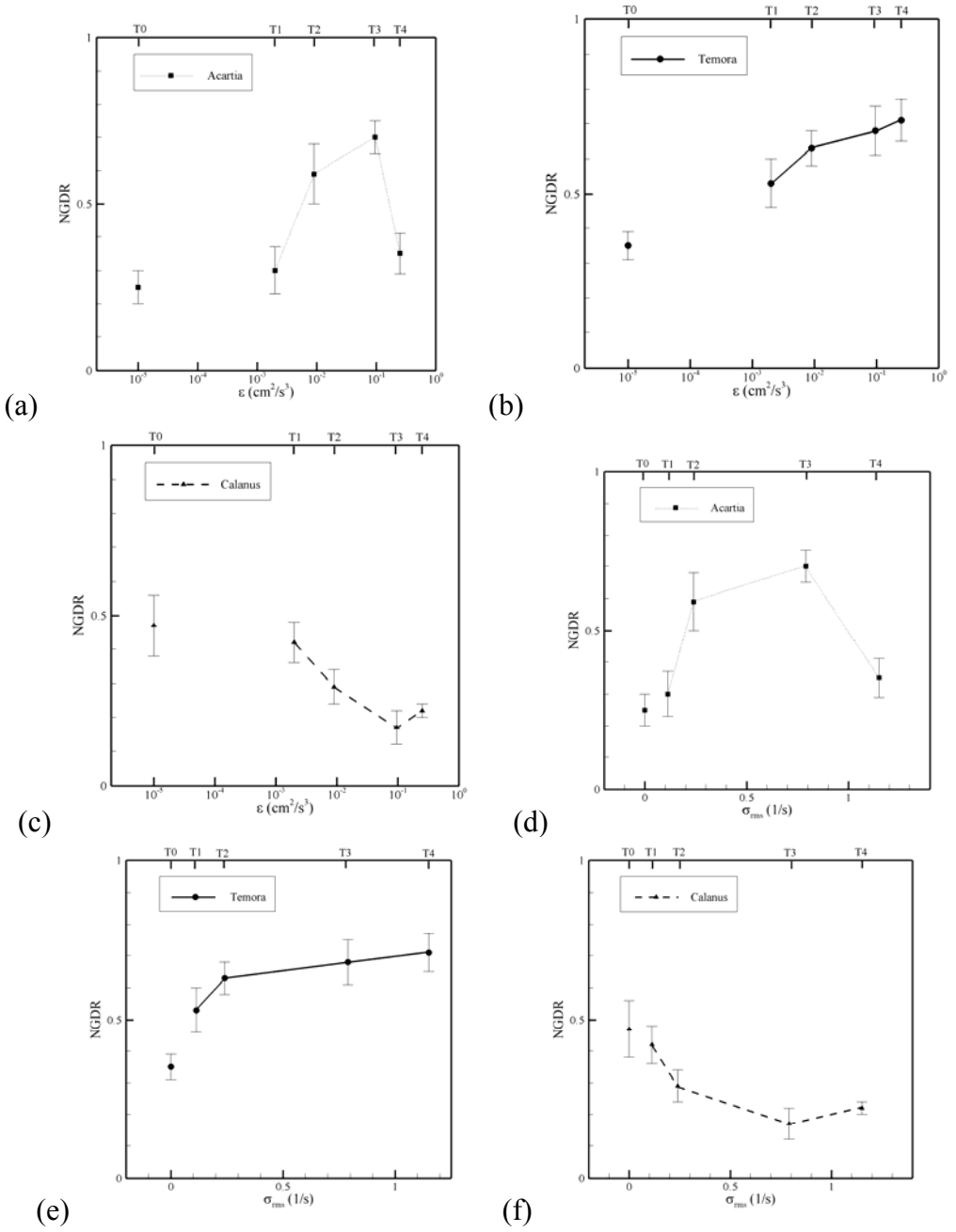

Figure 4.27 Net-to-gross-displacement ratio for (a), (b) *Acartia tonsa*, (c), (d) *Temora longicornis*, and (e), (f) *Calanus finmarchicus* as a function of turbulence intensity.

Table 4.4 shows the results for the Student Newman-Keuls test for NGDR. With increasing turbulence, the NGDR increased and then decreased for *A. tonsa* with the maximum occurring at T3. The NGDR for T0, T1, and T4 were coincident and significantly lower than the NGDR for T2 and T3. The dome shape trend is similar to the shape of the relative swim speed plot for *A. tonsa*. The NGDR for T3 was significantly lower than that of T1 for *C. finmarchicus*. Otherwise, the data points for *C. finmarchicus* were statistically coincident. *T. longicornis* trajectories became straighter with increased turbulence. The NGDR for T0 was significantly lower than that of the other T-levels, which were statistically coincident. For each species, there is variability among individuals, of course. Examples of an *A. tonsa* meandering trajectory and a straighter trajectory are plotted in Figures 4.5 and 4.7, respectively. An example of a straighter *T. longicornis* trajectory is plotted in 4.10.

The F-test was used to statistically determine the shape of the standard deviation, relative swim speed, and NGDR plots. SigmaPlot fit corresponding linear and quadratic regressions to the data for each species. An F-test compared the significance between the linear regression and the quadratic regression. The null hypothesis was that the quadratic regression was significantly better. A test statistic was computed and compared to the Critical F value. When the test statistic was greater than the Critical F, the quadratic regression was a significantly better fit. The results indicate a quadratic regression is significantly better than a linear regression only for *A. tonsa* NGDR and *C. finmarchicus* relative swim speed (Table 4.5).

Table 4.4 Results of Student Newman-Keuls test for NGDR. Rejection indicates a significant difference, whereas acceptance indicates there is not enough evidence to conclude the data sets are different.

(a) *A. tonsa*

Comparison	q	$q_{0.05,\nu,p}$	Conclusion
T3 v. T0	7.60	4.04	Reject
T3 v. T1	5.88	3.79	Reject
T3 v. T4	4.59	3.44	Reject
T3 v. T2	1.12	3.86	Accept
T3 v. T0	5.20	4.04	Reject
T3 v. T1	3.89	3.79	Reject
T2 v. T4	2.60	3.44	Accept
T4 v. T0	3.32	4.04	Accept
T4 v. T1	1.79	3.79	Accept
T1 v. T0	1.30	4.04	Accept

(b) *T. longicornis*

T3 v. T0	6.01	3.98	Reject
T3 v. T1	1.76	3.74	Accept
T3 v. T2	0.60	3.40	Accept
T3 v. T4	0.45	2.83	Accept
T4 v. T0	6.04	3.98	Reject
T4 v. T1	1.41	3.74	Accept
T4 v. T2	0.12	3.40	Accept
T2 v. T0	6.44	3.98	Reject
T2 v. T1	1.42	3.74	Accept
T1 v. T0	4.74	3.98	Reject

(c) *C. finmarchicus*

T1 v. T3	5.99	4.04	Reject
T1 v. T4	3.73	3.79	Reject
T1 v. T2	2.74	3.44	Accept
T1 v. T0	0.90	3.86	Accept
T0 v. T3	3.42	4.04	Accept
T0 v. T4	2.55	3.79	Accept
T0 v. T2	0.85	3.44	Accept
T2 v. T3	3.70	4.04	Accept
T2 v. T4	2.30	3.79	Accept
T4 v. T3	0.02	4.04	Accept

Table 4.5 Results of statistical regression test. An affirmative significant conclusion indicates that the quadratic regression is significantly better than the linear regression.

(a) *A. tonsa*

	Linear Regression	Quadratic Regression	Test Statistic	Critical F	Significant Conclusion
Standard Deviation	r^2=0.05 y=0.63+0.14x	r^2=0.05 $y=0.56+0.86x-0.63x^2$	0.38	4.02	No
Relative Swim Speed	r^2=0.19 y=0.88-0.49x	r^2=0.49 $y=0.62+2.2-2.4x^2$	3.30	4.02	No
NGDR	r^2=0.093 y=0.49+0.22x	r^2=0.42 $y=0.32+2.0x-1.5x^2$	6.61	4.02	Yes

(b) *T. longicornis*

	Linear Regression	Quadratic Regression	Test Statistic	Critical F	Significant Conclusion
Standard Deviation	r^2=0.01 y=0.27+0.03x	r^2=0.01 $y=0.26+0.13x-0.09x^2$	-0.16	3.98	No
Relative Swim Speed	r^2 = 0.32 y = 0.79-0.57x	r^2=0.35 $y=0.71+0.13x-0.16x^2$	-11.45	3.98	No
NGDR	r^2=0.098 y=0.753+0.29x	r^2=0.21 $y=0.59+1.7x-1.2x^2$	0.56	3.98	No

(c) *C. finmarchicus*

	Linear Regression	Quadratic Regression	Test Statistic	Critical F	Significant Conclusion
Standard Deviation	r^2=0.28 y=0.40+0.72x	r^2=0.51 $y=0.08+3.3x-2.5x^2$	-1.14	4.02	No
Relative Swim Speed	r^2=0.001 y=0.76+0.06x	r^2=0.33 $y=0.32+3.7x-3.4x^2$	9.42	4.02	Yes
NGDR	r^2=0.25 y=0.69-0.52x	r^2=0.27 $y=0.76-1.1x+0.53x^2$	-6.78	4.02	No

4.4 Copepod Escape Behavior

Another point of analysis was to determine how escape reactions change as a function of turbulence and species. Zooplankton are known to exhibit escape reactions from predators (Yen and Fields 1992). The escape reaction is most likely the best anti-predatory strategy for copepods (Fields and Yen 1997) though Hwang et al. (1994) showed short term increases in hop frequency with onset of turbulence. Escape responses were measured by randomly choosing individual copepods and counting the number of escapes they exhibit during 5-second intervals. A total of 200 5-second intervals were evaluated for the escape analysis for each turbulence level. The question to be answered is how turbulence affects the copepods' escape reaction.

A. tonsa is a hop and sink traveler (Mauchline 1998), therefore, more escapes were expected for *A. tonsa* than the other tested species. An escape is characterized by an abrupt and sudden movement by the copepod. An escape may resemble a jump or a quick dive. A sample trajectory demonstrating escape behavior is presented in Figure 4.4. This trajectory has two distinct escapes and three sinks; therefore, the copepod exhibited its typical swim style for T0. A sample *A. tonsa* trajectory for T1 shows an escape followed by a period of swimming (Figure 4.5). A sample T2 trajectory for *A. tonsa* shows a swim and escape pattern (Figure 4.6). For turbulence levels T3 and T4, *A. tonsa* was typically carried by the flow field. Example trajectories are plotted in Figures 4.7 and 4.8. The typical hop and sink behavior is not observed.

A. tonsa exhibited escape behavior more often for all turbulence levels than *C. finmarchicus* and *T. longicornis* (Figure 4.28). *A. tonsa* exhibited the most escapes for T1 (3.3 escapes/5-sec/copepod). The velocity fluctuation structure may mimic prey or

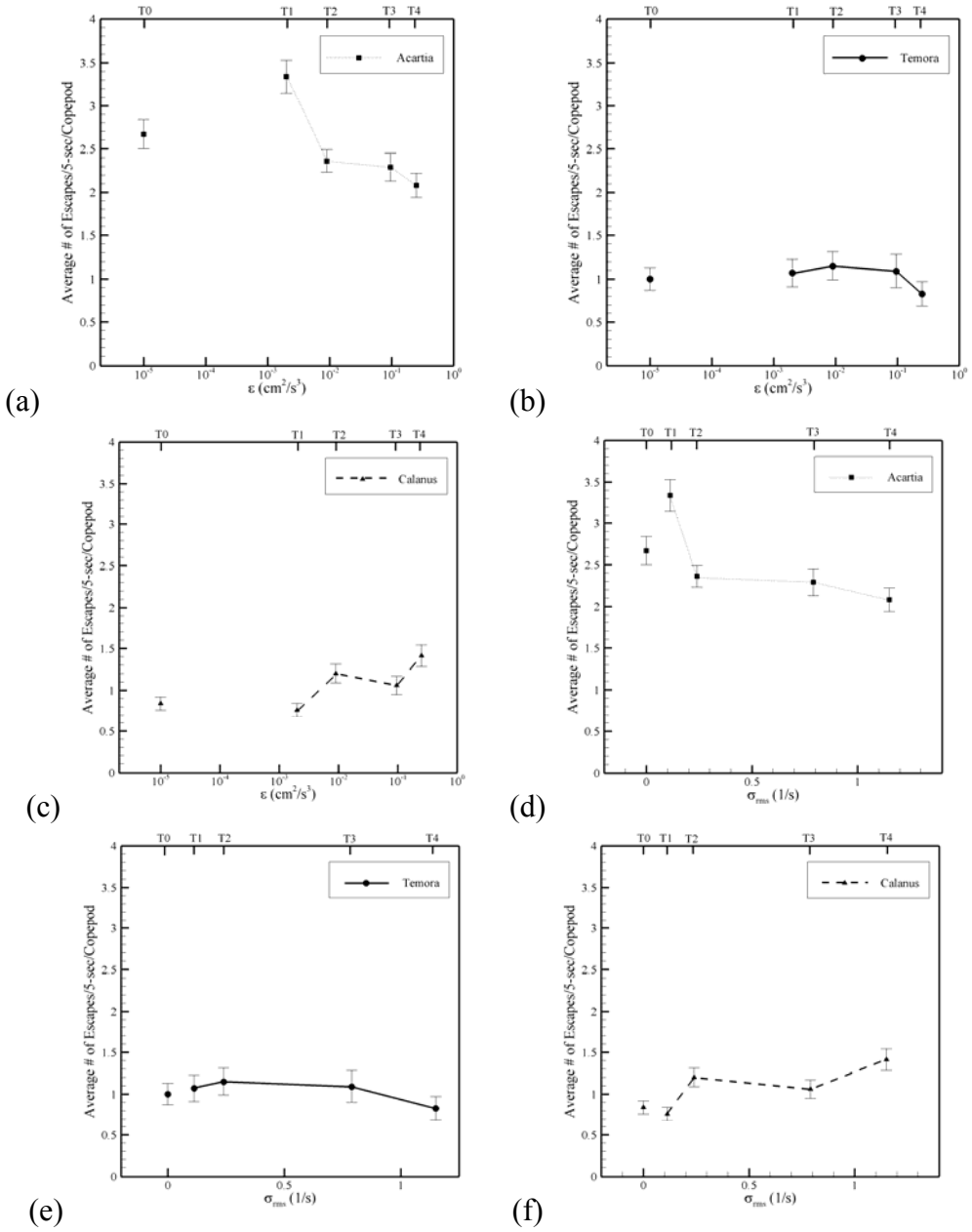

Figure 4.28 Number of escapes per 5-second interval per organism for (a), (b) *Acartia tonsa*, (c), (d) *Temora longicornis*, and (e), (f) *Calanus finmarchicus* as a function of turbulence intensity.

predators, thus inducing the escape reaction. Fields and Yen (1997) state that most copepods exhibit an escape reaction to an apparent predation risk. Copepods exhibit more escapes due to high strain rate as opposed to high fluid velocity (Fields and Yen 1997). Kiørboe et al. (1999) found that for *A. tonsa*, vorticity and acceleration signals did not elicit escape responses; however, fluid deformation, as quantified by strain rate, was the component of a velocity gradient that most generally caused escape reactions.

Saiz and Alcarez (1992) found that the escape frequency of *Acartia clausi* was higher in turbulent flow than in stagnant flow. This agrees with the current findings for *A. tonsa*. *A. clausi* exhibited sinking and rapid upward bursts of swimming to maintain their position in stagnant conditions (Saiz and Alcarez 1992). When turbulence was initiated the behavior was similar, but the frequency and velocity of the escapes increased.

T. longicornis and *C. finmarchicus* are cruise and sink travelers (Mauchline 1998). Sample *T. longicornis* trajectories are plotted in Figures 4.9 to 4.15. The sample T0 trajectory (Figure 4.9) shows an escape and swim pattern, while the sample T1, T2, T3, and T4 trajectories show typical cruise swim behavior for *T. longicornis*. The frequency of escapes for *T. longicornis* fluctuated around 1 escapes/5-sec/copepod for all the turbulence levels (Figure 4.28). Figures 4.16 to 4.20 show sample *C. finmarchicus* trajectories. All except for the T1 trajectory show the typical cruising swim style of *C. finmarchicus*. The T1 sample trajectory (Figure 4.17) shows *C. finmarchicus* escape behavior. *T. longicornis* and *C. finmarchicus* did not exhibit the escape (hopping) behavior similar to *A. tonsa*. While the escape frequency of *T. longicornis* was fairly

constant for each turbulence level, the escape frequency for *C. finmarchicus* increased slightly with turbulence intensity.

Standard error was calculated for escape frequency as a function of the number of copepod 5-second intervals for. When standard error leveled off, the escape frequency had statistically converged. Figure 4.29 is an example standard error trend for *Acartia tonsa* for T1.

Table 4.6 shows the results of the Student Newman-Keuls test for escape reactions. There was a significant increase between the T1 data set and the other T-levels for *A. tonsa*, which were statistically coincident. There was a significant difference between the escape data sets for T4 versus T0 and T1 data sets for *C. finmarchicus*. Otherwise, *C. finmarchicus* escape reactions were statistically coincident between T-levels. There were no significant differences between the pairwise comparisons for *T. longicornis* escape data sets. It can be concluded that between T-levels, *T. longicornis* exhibited consistent escape reactions.

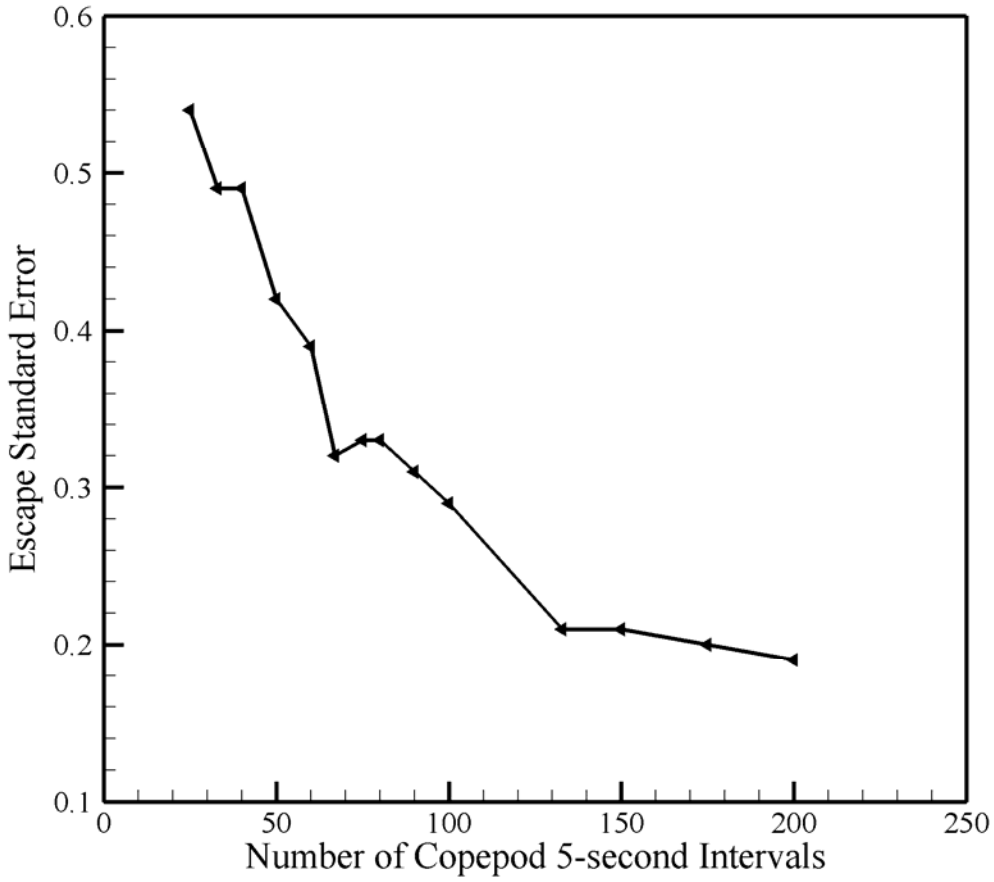

Figure 4.29 Standard error of escape data as a function of the number of copepod 5-second intervals for *Acartia tonsa* for T1.

Table 4.6 Results of Student Newman-Keuls test for escapes. Rejection indicates a significant difference, whereas acceptance indicates there is not enough evidence to conclude the data sets are different.

(a) *A. tonsa*

Comparison	q	$q_{0.05,\nu,p}$	Conclusion
T1 v. T4	7.95	3.86	Reject
T1 v. T3	6.62	3.63	Reject
T1 v. T2	6.18	3.31	Reject
T1 v. T0	4.23	2.77	Reject
T0 v. T4	3.72	3.86	Accept
T0 v. T3	2.40	3.63	Accept
T0 v. T2	1.96	3.31	Accept
T2 v. T4	1.77	3.86	Accept
T2 v. T3	0.44	3.63	Accept
T3 v. T4	1.32	3.86	Accept

(b) *T. longicornis*

T2 v. T4	2.03	4.04	Accept
T2 v. T0	0.95	3.79	Accept
T2 v. T1	0.51	3.44	Accept
T2 v. T3	0.38	3.86	Accept
T3 v. T4	1.65	4.04	Accept
T3 v. T0	0.57	3.79	Accept
T3 v. T1	0.13	3.44	Accept
T1 v. T4	1.52	4.04	Accept
T1 v. T0	0.44	3.79	Accept
T0 v. T4	1.08	4.04	Accept

(c) *C. finmarchicus*

T4 v. T1	6.28	3.86	Reject
T4 v. T0	5.51	3.63	Reject
T4 v. T3	3.40	3.31	Reject
T4 v. T2	2.01	2.77	Accept
T2 v. T1	4.26	3.86	Reject
T2 v. T0	3.50	3.63	Accept
T2 v. T3	1.39	3.31	Accept
T3 v. T0	2.87	3.86	Accept
T3 v. T1	2.11	3.63	Accept
T0 v. T1	0.77	3.86	Accept

4.5 Summary of Results

Based on the sample trajectories, aggregation behavior, swim speed analysis, and NGDR, there are important conclusions about the effect of laboratory turbulence on copepods. The size of the copepod has a significant effect on its aggregation and swimming capability with increasing turbulence. The smaller copepods had less ability to overcome a strong flow field, and they were more likely to be advected by the stronger flow fields. Swim style also can influence how a copepod reacts to increased turbulence. If the copepod is a hop and sink traveler, then the copepod continues to hop and sink more than its cruising counterparts as turbulence increases. The cruise and sink travelers did not alter the number of escapes in response to turbulence, although *C. finmarchicus* slightly increased the number of escapes for T4.

CHAPTER V

CONCLUSIONS AND RECOMMENDATIONS

The turbulence generator described by Brathwaite (2003) and Webster et al. (2004) was used to study the behavioral effects of laboratory turbulence on three species of copepods, *Acartia tonsa*, *Temora longicornis*, and *Calanus finmarchicus*. Each species was exposed to stagnant water plus four levels of turbulence intensity. The turbulence characteristics previously have been stochastically described as nearly isotropic and homogeneous in the apparatus center where the behavioral observations are made. The copepods' aggregation behavior, trajectory patterns, escape reactions, and net-to-gross-displacement ratio were analyzed.

The copepods were recorded by two cameras focused on the center of the box and viewing the observation region from orthogonal perspectives. Three-dimensional trajectories of individual copepods were subsequently determined by combining the orthogonal video recordings.

A green laser beam was used to attract the copepods to the vertical center of the box and assisted in studying the aggregative ability of the copepods. The phototactic aggregation behavior was analyzed by counting the number of copepods near the laser beam per minute for each turbulence level. The results suggest that the size of copepod was important. The smaller species, *A. tonsa* and *T. longicornis*, became more numerous as the turbulence increased, suggesting that they are advected and mixed by the turbulent flow motion. Conversely, *C. finmarchicus*, the larger species, was more numerous at low

levels of turbulence. *T. longicornis* showed a positive phototactic response to the laser light, but as turbulence intensity increased its ability to aggregate to the light source diminished. *C. finmarchicus* and *A. tonsa* are known to be phototactic, although this was not explicitly observed in the T-box experiments. The time of day, stomach fullness, or quality of light could have played a role in their phototactic reaction.

Swimming speed analysis suggested a changing mode of transportation for increasing turbulence. The relative swim speed of all three species was highest at T2. At the highest turbulence intensity the relative swim speed approached zero indicating that the copepods were being transported by the flow rather than swimming by their own locomotion. *C. finmarchicus*, the largest copepod tested, had the highest relative swim speed at T4, and *A. tonsa*, the smallest copepod tested, had the lowest. Hence, the larger copepod was able to swim against the fluctuating fluid motion to some degree, while the smallest copepod was essentially transported by the flow with little independent motion.

Net-to-gross-displacement ratio measured the tortuousity of the trajectories. *T. longicornis's* trajectories became straighter, whereas *C. finmarchicus* became more tortuous with increasing turbulence. *A. tonsa* trajectories became straighter with increased turbulence until T4 where they were more meandering. The more tortuous paths might be because the flow field is containing them in a smaller volume for a longer time.

The escape behavior was analyzed by counting the number of escapes of individual copepods per five second interval. It was found that *A. tonsa* escaped more frequently for all turbulence intensity levels than *C. finmarchicus* and *T. longicornis*. This was explained due to the fact that *A. tonsa* is a hop and sink traveler, while *C.*

finmarchicus and *T. longicornis* are cruise and sink travelers. *A. tonsa* and *C. finmarchicus* had the highest escape frequency at T1 and T4, respectively. The turbulent flow fluctuations may mimic the disturbance created by their prey or predators, thereby inducing an escape reaction. *T. longicornis* did not have a substantial variation of escape reactions across the turbulence intensity levels.

Detailed analysis of copepod trajectories has demonstrated that the size and swimming style of the copepod were important when determining how they behave in turbulent waters. The smaller copepods were more likely to be controlled by the water movement as opposed to swimming through the flow. Larger copepods were stronger and could swim through more turbulent flow fields. They are less affected by the higher velocities and shear stress.

Additional experiments are recommended to further test copepod response to turbulent flow motions. Additional experiments comparing copepods of different size or copepods with hop-sink versus cruise swimming styles would test the following hypothesis: Variations in copepod response to turbulence are due to size and swimming style, as suggested by the results. Experiments comparing copepod behavior at different months of the year would test the following hypothesis: Variations in copepod response to turbulence are due to activity during different months. For example, during mating season, copepods might be more active. By testing the copepods at different hours of the day, the following hypothesis could be tested: Variations in copepod response are due to diel migration to the surface at dusk and dawn. By testing copepods before and after feeding would also test the hypothesis of diel migration. Some copepods migrate to the surface to feed at dusk and dawn and then sink to lower depths when full. Experiments

on copepods with empty versus full stomachs would test the following hypothesis: Variations in copepod response are due to a difference in stomach fullness. Most importantly, it would be highly desirable to measure the instantaneous flow field in the region surrounding the copepod in order to directly correlate velocity fluctuations to animal behavior.

REFERENCES

Ambler, J.W., Ferrari, F.D., and Fornshell, J.A. (1991) "Population structure and swarm formation of the cyclopoid copepod *Dioithona oculata* near mangrove cays," *Journal of Plankton Research* 13, 1257-1272.

Apstein, C. (1910) "Hat ein Organismus in der tiefe gelebt, in der er gefischt ist?" *Internationale Revue der gesamten Hydrobiologie und Hydrographie* 3, 17-33.

Brathwaite, A. (2003) "A novel apparatus for simulating isotropic oceanic turbulence at low Reynolds number," M.S. Thesis, Georgia Institute of Technology.

Buskey, E.J., and Swift, E. (1983) "Behavioral responses of the coastal copepod *Acartia hudsonica* (Pinhey) to simulated dinoflagellate bioluminescence," *Journal of Experimental Marine Biology and Ecology* 72, 43-58.

Buskey, E.J., and Swift, E. (1985) "Behavioral responses of oceanic zooplankton to simulated biolumincescence," *Biological Bulletin* 168, 263-275.

Buskey, E.J., Mann, C.G., and Swift, E. (1986) "The shadow response of the estuarine copepod *Acartia tonsa* (Dana)," *Journal of Experimental Marine Biology andEcology* 103, 65-75.

Buskey, E.J., Baker, K.S., Smith, R.C., and Swift, E. (1989) "Photosensitivity of the oceanic copepods *Pleuromamma gracilis* and *Pleuromamma xiphias* and its relationship to light penetration and daytime depth distribution," *Marine Ecology Progress Series* 55, 207-216.

Buskey, E.J., Coulter, C., and Strom, S. (1993) "Locomotory patterns of microzooplankton: Potential effects on food selectivity of larval fish," *Bulletin of Marine Science* 53, 29-43.

Buskey, E.J. (1994) "Factors affecting feeding selectivity of visual predators on the copepod *Acartia tonsa*: locomotion, visibility and escape responses," *Hydrobiologia* 292/293, 447-453.

Cohen, J.H., and Forward Jr., R.B. (2002) "Spectral sensitivity of vertically migrating marine copepods," *Biological Bulletin* 203, 307-314.

Fields, D.M. and Yen, J. (1996) "The escape behavior of *Pleuromamma Xiphias* in response to a quantifiable fluid mechanical disturbance," in *Zooplankton: Sensory Ecology and Physiology*, Vo1. 1, Lenz, P.H., Hartline, D.K., Purcell, J.E., and MacMillan, D.L. [eds.], Gordon and Breach Publishers, Amsterdam, pp. 323-339.

Fields, D.M., and Yen, J. (1997) "The escape behavior of marine copepods in response to a quantifiable fluid mechanical disturbance," *Journal of Plankton Research* 19, 1289-1304.

Fields, D.M., Shaeffer, D.S., and Weissburg, M.J. (2002) "Mechanical and neural responses from the mechanosensory hairs on the antennule of *Gaussia princeps*," *Marine Ecology Progress Series* 227, 173-186.

Franks, P.J.S. (2001) "Turbulence avoidance: An alternate explanation of turbulence-enhanced ingestion rates in the field," *Limnology and Oceanography* 46, 959-963.

Gallager, S.M., Yamazaki, H., and Davis, C. S. (2004) "Contribution of fine-scale vertical structure and swimming behavior to formation of plankton layers on Georges Bank," *Marine Ecology Progress Series* 267, 27-43.

Gross, F., and Raymont, J.E.G. (1942) "The specific gravity of *Calanus finmarchicus*," *Proceedings of the Royal Society of Edinburgh* 61B, 288-296.

Hirche, H.-J. (1987) "Temperature and plankton. II. Effect on respiration and swimming activity in copepods from the Greenland Sea," *Marine Biology* 94, 347-356.

Hwang, J.-S., Costello, J.H., and Strickler, J.R. (1994) "Copepod grazing in turbulent flow: Elevated foraging behavior and habituation of escape reactions," *Journal of Plankton Research* 16, 421-431.

Incze, L.S., Hebert, D., Wolff, N., Oakey N., and Dye, D. (2001) "Changes in copepod distributions associated with increased turbulence from wind stress," *Marine Ecology Progress Series* 213, 229-240.

Jacobs, J. (1961) "Laboratory cultivation of the marine copepod *Pseudodiaptomus cornatus*," *Limnology and Oceanography* 6, 443-446.

Jiminez, J. (1997) "Oceanic turbulence at millimeter scales," *Scientia Marina* 61, 47-56.

Jonsson, Per R. and Tiselius, P. (1990) "Feeding behavior, prey detection and capture efficiency of the copepod *Acartia tonsa* feeding on planktonic ciliates," *Marine Ecology Progress Series* 60, 35-44.

Kiørboe, T., and Saiz, E. (1995) "Planktivorous feeding in calm and turbulent environments, with emphasis on copepods," *Marine Ecology Progress Series* 122, 135-145.

Kiørboe, T., Saiz, E., and Visser, A.W. (1999) "Hydrodynamic signals perception in the copepod *Acartia tonsa*," *Marine Ecology Progress Series* 179, 97-111.

Kiørboe, T., and Visser, A.W., (1999) "Predator and prey perception in copepods due to hydromechanical signals," *Marine Ecology Progress Series* 179, 81-95.

Lagadeuc, Y., Boule, M., and Dodson, J.J. (1997) "Effect of vertical mixing on the vertical distribution of copepods in coastal waters," *Journal of Plankton Research* 19, 1183-1204.

Leising, A.W., and Yen, J. (1997) "Spacing mechanisms within light-induced copepod swarms," *Marine Ecology Progress Series* 155, 127-135.

Mackas, D.L., Sefton, H., Miller, C.B., and Raich, A. (1993) "Vertical partitioning by large calanoid copepods in the oceanic subarctic Pacific during Spring," *Progress in Oceanography* 32, 259-294.

Mann, K.H., and Lazier, J.R.N. (1996) *Dynamics of Marine Ecosystems*, Blackwell Scientific Publications, Boston, MA.

Mauchline, J. (1998) *The Biology of Calanoid Copepods*, Blaxter, Academic Press, London.

Rothschild, B.J., and Osborn, T.R. (1988) "Small-scale turbulence and plankton contact rates," *Journal of Plankton Research* 10, 465-474.

Saiz, E., and Alcarez, M. (1992) "Free-swimming behavior of *Acartia clausi* (Copepoda: Calanoida) under turbulent water movement," *Marine Ecology Progress Series* 80, 229-236.

Saiz, E. (1994) "Observations of the free-swimming behavior of *Acartia tonsa*: Effects of food concentration and turbulent water motion," *Limnology and Oceanography* 39, 1566-1578.

Saiz, E., and Kiørboe, T. (1995) "Predatory and suspension feeding of the copepod *Acartia tonsa* in turbulent environments," *Marine Ecology Progress Series*, 122, 147-158.

Saiz, E., Calbet, A., and Broglio, E. (2003) "Effects of small-scale turbulence on copepods: The case of *Oithona davisae*," *Limnology and Oceanography* 48, 1304-1311.

Shallek, W. (1942) "The vertical migration of the copepod *Acartia tonsa* under controlled illumination," *Biological Bulletin* 82, 112-126.

Shallek, W. (1943) "The reaction of certain Crustacia to direct and diffuse light," *Biological Bulletin* 84, 98-105.

Simard, Y., Lacroix, G., and Legendre, L. (1985) "In situ twilight grazing rhythm during diel vertical migrations of a scattering layer of *Calanus finmarchicus*," *Limnology and Oceanography* 30, 598-606.

Stearns, D.E., and Forward Jr., R.B. (1984) "Photosensitivity of the calanoid copepod *Acartia tonsa*," *Marine Biology* 82, 85-89.

Tiselius, P. (1992) "Behavior of *Acartia tonsa* in patchy food environments," *Limnology and Oceanography* 37, 1640-1651.

Titelman, J. (2001) "Swimming and escape behavior of copepod nauplii: Implications for predator-prey interactions among copepods," *Marine Ecology Progress Series* 213, 203-213.

Titelman, J., and Kiørboe, T. (2003) "Motility of copepod nauplii and implications for food encounter," *Marine Ecology Progress Series* 247, 123-135.

Titelman, J., and Kiørboe, T. (2003) "Predator avoidance by nauplii," *Marine Ecology Progress Series* 247, 137-149.

Viitasalo, M., Kiørboe, T., Flinkman, J., Pederson, L.W., and Visser, A.W. (1998) "Predation vulnerability of planktonic copepods: consequences of predator foraging strategies and prey sensory abilities," *Marine Ecology Progress Series* 175: 129-142.

Visser, A.W., Saito, H., Saiz, E., Kiørboe, T. (2001) "Observations of copepod feeding and vertical distribution under natural turbulent conditions in the North Sea," *Marine Biology* 138, 1011-1019.

Visser, A.W., and Stips, A. (2002) "Turbulence and zooplankton production: Insights from PROVESS," *Journal of Sea Research* 47, 317-329.

Webster, D.R., Brathwaite, A., and Yen, J. (2004) "A novel apparatus for simulating isotropic oceanic turbulence at low Reynolds number," *Limnology and Oceanography: Methods* 2, 1-12.

Yamazaki, H., and Squires, K.D. (1996) "Comparison of oceanic turbulence and copepod swimming," *Marine Ecology Progress Series* 144, 299-301.

Yamazaki, H., Mackas, D.L., and Denman, K.L. (2002) "Coupling small-scale physical processes with biology," *The Sea*, Vol. 12, Robinson, A.R., McCarthy, J.J., and Rothschild, B.J. [eds.], John Wiley & Sons, New York, pp. 51-111.

Yen, J., and Fields, D.M. (1992) "Escape responses of *Acartia hudsonica* (Copepoda) nauplii from the flow field of *Temora longicornis* (Copepoda)," *Arch. Hydrobiol. Beih.* 36, 123-134.

Yen, J., and Strickler, J.R. (1996) "Advertisement and concealment in the plankton: What makes a copepod hydrodynamically conspicuous?" *Invertebrate Biology* 115(3), 191-205.

Yen, J., and Bundock, E.A. (1997) "Aggregative behavior in zooplankton: Phototactic swarming in four developmental stages of *Coullana Canadensis* (Copepoda, Harpacticoida)," *Animals Groups in Three Dimensions*, Parish, J. and Hamner, W. [eds.], Cambridge University Press, New York, pp. 143-162.

Zar, J.H. (1999) *Biostatistical analysis*, 4th Edition, Prentice Hall, Upper Saddle River, N.J.